

COMPLEX ZNN FOR COMPUTING TIME-VARYING WEIGHTED PSEUDO-INVERSES

*Predrag S. Stanimirović, Xue-Zhong Wang, Haifeng Ma**

We classify, extend and unify various generalizations of weighted Moore-Penrose inverses in indefinite inner product spaces. New kinds of generalized inverses are introduced for this purpose. These generalized inverses are included in the more general class called as the weighted indefinite pseudoinverses (WIPI), which represents an extension of the Minkowski inverse (MI), the weighted Minkowski inverse (WMI), and the generalized weighted Moore-Penrose (GWM-P) inverse. The WIPI generalized inverses are introduced on the basis of two Hermitian invertible matrices and two Hermitian involutory matrices and represented as particular outer inverses with prescribed ranges and null spaces, in terms of appropriate full-rank and limiting representations. Application of introduced generalized inverses in solving some indefinite least squares problems is considered. New Zeroing Neural Network (ZNN) models for computing the WIPI are developed using derived full-rank and limiting representations. The convergence behavior of the proposed ZNN models is investigated. Numerical simulation results are presented.

1. INTRODUCTION

The indefinite inner product associated with an invertible Hermitian matrix J is defined by

$$\langle u, v \rangle_J = (u, Jv) = u^* Jv,$$

where $(x, y) = x^*y$ denotes the conventional inner product in a Hilbert (unitary) space. An indefinite inner product (IIP) space denotes a vector space equipped with

*Corresponding author. Haifeng Ma (haifengma@aliyun.com)

2010 Mathematics Subject Classification. 15A09, 65F20, 68T05.

Keywords and Phrases. Weighted Minkowski inverse; indefinite inner product; Zhang neural network; outer inverse; time-varying complex matrix.

an indefinite inner product defined in terms of an invertible Hermitian matrix J . In the literature, it is frequently assumed that J belongs to the class of Hermitian involutory matrices, which satisfy properties

$$(1) \quad J^* = J, \quad J^2 = I.$$

Some classes of Hermitian involutory matrices were highlighted in [23]. In order to clarify the presentation, the weight matrix J of the order n is denoted as J_n . Peng and Hu in [22] discovered that any square matrix $J_n \in \mathbb{C}^{n \times n}$ satisfying (1) is diagonalizable in the form

$$(2) \quad J_n = S_n I_{k,n-k} S_n^*, \quad q \leq n,$$

where S_n is a unitary $n \times n$ matrix and

$$(3) \quad I_{k,n-k} = \pm \begin{bmatrix} I_k & 0 \\ 0 & -I_{n-k} \end{bmatrix} = I_{k,n-k} \in \mathbb{C}^{n \times n}, \quad k \leq n,$$

denotes the $(k, n-k)$ signature matrix, assuming that I_n is the $n \times n$ identity matrix. The concept of the adjoint in an IIP space can be introduced using an indefinite inner product which includes two vectors $x \in \mathbb{C}^n, y \in \mathbb{C}^m$ and two appropriate Hermitian invertible matrices J_m, J_n as follows

$$(4) \quad \langle Ax, y \rangle_{J_m} = (Ax, J_m y) = (x, A^* J_m y) = (x, J_n (J_n A^* J_m) y) = (x, J_n A^\sim y) = \langle x, A^\sim y \rangle_{J_n},$$

where A^* denotes the usual conjugate and transpose matrix of A . As a consequence, the matrix

$$A^\sim = J_n A^* J_m \in \mathbb{C}^{n \times m}$$

is called the adjoint of A (relative to J_m, J_n). If J_m, J_n are signature matrices $J_m = I_{p,m-p}, J_n = I_{q,n-q}$, then A^\sim is called a *pseudo-Euclidean conjugate transpose* of A , defined in [9]. Further, the weight tensors $J_m = I_{1,m-1}$ and $J_n = I_{1,n-1}$ define the Minkowski inner product and Minkowski conjugate transpose (see, for example [9, 26]). Particularly, a space with the Minkowski inner product is called the Minkowski space, and denoted by \mathcal{M} .

The *weighted adjoint* matrix can be introduced using an indefinite inner product which includes two vectors $x \in \mathbb{C}^n, y \in \mathbb{C}^m$, two appropriate Hermitian involutory matrices J_m, J_n and two Hermitian invertible matrices M, N of appropriate dimensions:

$$(5) \quad \begin{aligned} \langle Ax, y \rangle_{J_m M} &= (Ax, J_m M y) = (x, A^* J_m M y) = (x, J_n N (N^{-1} J_n A^* J_m M) y) \\ &= \langle x, A^\approx y \rangle_{J_n N}, \end{aligned}$$

where the weighted adjoint matrix A^\approx of A is defined as

$$(6) \quad A^\approx = N^{-1} A^\sim M = N^{-1} J_n A^* J_m M.$$

In the case when J_m, J_n are appropriate signature matrices $J_m = I_{p, m-p}, J_n = I_{q, n-q}$, the weighted adjoint matrix becomes the *weighted pseudo-Euclidean conjugate transpose* matrix. Particularly, the choice $p = q = 1$ gives the *weighted Minkowski conjugate transpose* matrix, considered in [9, 53]. In the special case $J_m = I_m, J_n = I_n$, the weighted adjoint matrix becomes the *MN*-adjoint, considered in [13].

For any matrix A of the order $m \times n$ the following analogies of Penrose equations can be considered in IIP spaces:

$$(1) \quad AXA = A, \quad (2) \quad XAX = X, \quad (3^{\sim}) \quad (AX)^{\sim} = AX, \quad (4^{\sim}) \quad (XA)^{\sim} = XA \\ (3^{\approx}) \quad (AX)^{\approx} = AX, \quad (4^{\approx}) \quad (XA)^{\approx} = XA.$$

The generalized inverses obeying the equations defined by the numbers contained in a sequence \mathcal{S} of elements from the set $\{1, 2, 3^{\sim}, 4^{\sim}, 3^{\approx}, 4^{\approx}\}$ is denoted by $A\{\mathcal{S}\}$. A generalized inverse from $A\{\mathcal{S}\}$ is called an \mathcal{S} -inverse of A . The matrix X satisfying the equations (1), (2), (3^{\sim}) , (4^{\sim}) represents the Moore-Penrose inverse in IIP spaces. We use the term *indefinite pseudoinverse* (IPI shortly) to denote such the matrix X and mark it by A^{\odot} . In the IIP space where J_n and J_m are appropriate signature matrices, the IPI becomes the pseudo-Euclidean pseudoinverse (PPI shortly) of A , which is denoted by A^{\oplus} . In the Minkowski space (the case $k = 1$ of (3)), the pseudo-Euclidean inverse reduces to the Minkowski inverse $A^{\mathcal{M}}$. The weighted indefinite pseudoinverse (WIPI shortly), denoted by $A_{M,N}^{\odot}$, satisfies matrix equations (1), (2), (3^{\approx}) , (4^{\approx}) . In the case when J_m, J_n are signature matrices, the WIPI becomes the *weighted pseudo-Euclidean pseudoinverse* (WPPI shortly), which will be denoted by $A_{M,N}^{\oplus}$. Further, after the choice $k = 1$ of (3), the WPPI becomes the *weighted Minkowski inverse* (WMI shortly), which was defined in [9] and later investigated in [53]. The WMI is denoted in the present paper by $A_{M,N}^{\mathcal{M}}$ and related to M, N and Minkowski matrices J_n, J_m . Also, the Minkowski inverse (MI shortly) has been investigated in several articles. Some of them are, for example, [16, 20, 52]. Necessary and sufficient condition for the existence of the Minkowski inverse in the Minkowski space is stated in [20]. New representations, properties and conditions for the continuity of the weighted Minkowski inverse were considered in [9, 53]. The weighted Minkowski inverse is one of the important generalized inverses for solving matrix equations in Minkowski space [53]. The nonnegativity of the Moore-Penrose inverse of Gram matrices in an indefinite inner product space with the indefinite matrix multiplication was considered in [25]. Li et al. in [13] provided the mixed and componentwise condition numbers for the Moore-Penrose inverse in indefinite inner product spaces (IPI). Nonnegativity of the inverse, the Moore-Penrose inverse and other generalized inverses in indefinite inner product spaces was investigated in [7]. The matrix X is said to be Re-nnd (Re-nonnegative definite) if its Hermitian part $H(X) = \frac{1}{2}(X + X^*)$ is positive semidefinite, i.e., $H(X) \geq 0$. Necessary and sufficient conditions for the existence of Re-nnd solutions (resp. anti-reflexive solutions) of the equation $AXB = C$ in terms of Minkowski inverses were considered in [10] (resp. in [11]). Additive properties of the generalized Drazin inverse of sum $P + Q$ of two GD-Drazin invertible

operators P, Q in Minkowski space were investigated in [12].

Following the results from [8, 13] it is observable that the equations (3 \sim) and (4 \sim) can be rewritten in the equivalent form

$$\begin{aligned} (3\sim) \quad (AX)\sim = AX &\iff (J_m AX)^* = J_m AX; \\ (4\sim) \quad (XA)\sim = XA &\iff (XAJ_n)^* = XAJ_n. \end{aligned}$$

Similarly, the equations (3 \approx) and (4 \approx) can be rewritten as

$$\begin{aligned} (3\approx) \quad (AX)\approx = AX &\iff (J_m MAX)^* = J_m MAX; \\ (4\approx) \quad (XA)\approx = XA &\iff (J_n NXA)^* = J_n NXA. \end{aligned}$$

As a consequence, the generalized inverse $A_{M,N}^\odot$ in the case $J_m = I_m, J_n = I_n$ becomes the generalized weighted Moore-Penrose (GWM-P) inverse, investigated in [13, 28]. We use the term $A_{MN}^{(\dagger)}$ to denote the GWM-P inverse. Further, $A_{M,N}^\odot = A_{J_m M J_n N}^{(\dagger)}$. In addition, if M, N are positive definite matrices, then $A_{M,N}^\odot$ becomes the usual weighted Moore-Penrose inverse $A_{M,N}^\dagger$.

A summarization and classification of various various generalized inverses which satisfy all the matrix equations (1), (2), (3 \approx), (4 \approx) in a number of particular cases is presented in Table 1.

Table 1. Generalized inverses which satisfy (1), (2), (3 \approx), (4 \approx).

M, N	J_m, J_n	Name	Short	Notation
Hermitian invertible	Hermitian involutory	Weighted indefinite pseudoinverse	WIPI	$A_{M,N}^\odot$
I_m, I_n	Hermitian involutory	Indefinite pseudoinverse	IPI	A^\odot
Hermitian invertible	$I_{p,m-p}, I_{q,n-q}$	Weighted pseudo Euclidean pseudoinverse	WPPI	$A_{M,N}^\oplus$
I_m, I_n	$I_{p,m-p}, I_{q,n-q}$	Pseudo-Euclidean pseudoinverse	PPI	A^\oplus
Hermitian invertible	$I_{1,m-1}, I_{1,n-1}$	Weighted Minkowski inverse	WMI	$A_{M,N}^M$
I_m, I_n	$I_{1,m-1}, I_{1,n-1}$	Minkowski inverse	MI	A^M
Hermitian invertible	I_m, I_n	Generalized weighted Moore-Penrose inverse	GWM-P	$A_{MN}^{(\dagger)}$
Positive definite	I_m, I_n	Weighted Moore-Penrose inverse	WMP	A_{MN}^\dagger
I_m, I_n	I_m, I_n	Moore-Penrose inverse	MP	A^\dagger

Our first motivation was applicability of the PPI generalized inverses in solving various appearances of indefinite least-squares (ILS) problem. The ILS problems arise in robust estimation, filtering and control [2]. An algorithm for solving an ILS problem was investigated in [2]. Motivated by the applicability of various Pseudo-Euclidean inverses, we set itself two main goals. The first goal is a detailed investigation of the applicability of PPI generalized inverses in various ILS problems.

Our second goal is to define appropriate numerical algorithms for computing the WIPI in both time-invariant and time-varying case. To the best of our knowledge, only iterative methods for computing the weighted Minkowski inverse are considered so far. We observed four iterative methods defined in [9] as well as a family of iterative methods of the hyperposer type from [16] for approximating the weighted Minkowski inverse. These methods are iterative, suffering from the choice of the initial approximation which must satisfy rigorous and ultimate conditions. Moreover, these methods are appropriate only for time-invariant matrices. Our selection of an appropriate technique for computing WIPI, WPI and PI in time-invariant case is guided by the fact that many authors have shown great interest for computing the inverse or various classes of generalized inverses on the basis of gradient-based recurrent neural networks (GNNs) or Zhang neural networks (ZNNs). Recurrent neural networks (RNNs) show a significant advantage in comparison with the numerical iterative algorithms. Firstly, the main feature of RNNs is their ability of hardware implementation and parallel distributed essence of recurrent neural dynamics, which makes them applicable in time-varying case as well as in real-time applications [44]. Also, as it was shown in [46], the discrete-time ZNN model incorporates Newton iteration as its special case. As a further confirmation of this fact, we briefly restate main trends in this research. A number of nonlinear and linear recurrent neural network models for computing the inverse or the pseudoinverse were developed in [19, 33, 34]. Further, various RNNs designed for calculating the pseudoinverse of rank-deficient matrices were created in [36]. Three recurrent neural networks for computing the weighted Moore-Penrose inverse were introduced in [40]. A feed-forward neural network architecture for computing the Drazin inverse was proposed in [3]. The dynamic equation and induced gradient recurrent neural network for computing the Drazin inverse was defined in [30]. Gradient-based RNNs for generating outer inverses with prescribed range and null space in the time-invariant case were introduced in [55]. Two specific dynamic state equations and corresponding gradient based RNNs for generating the class of outer inverses of time-invariant real matrices were proposed in [31]. In [15], the authors defined five complex-valued ZNN models which are aimed to computation of time-varying complex matrix generalized inverses. ZNN models for online time-varying full-rank matrix pseudoinversion were introduced and analyzed in [43]. An RNN for computing the Drazin inverse with the linear activation function was proposed by Stanimirović, Živković, and Wei in [30]. The relationship between the Zhang matrix inverse and the Drazin inverse, discovered in [45], leads to the same dynamic state equation which was considered in [30] in the time invariant matrix case. The dynamical equation and corresponding artificial recurrent neural network for computing the Drazin inverse of an arbitrary square real matrix, without any restriction on eigenvalues of its rank invariant powers, were proposed in [29]. Zhang et al. in [47] introduced a general ZNN model for online inversion of time-varying matrices and its further verification was presented in [48]. Various ZNN models for computing online time-varying Moore-Penrose inverse of a full-rank matrix were proposed in [50]. Two ZNN models for computing the Drazin inverse of arbitrary time-varying or time-invariant complex square matrix were presented

in [37]. ZNN models for computing outer inverses with prescribed range and null space of time-varying complex matrix were presented recently in [38].

Our intention in the present paper is to derive appropriate ZNN models for computing the WIPI in the time-varying complex case. Particularly, provided ZNN models will be applicable in the computation of the generalized inverses WPPI, PPI, WMI and MI. The dynamics of these neural networks are based on matrix-valued ZFs arising from the limit representations of the WIPI. Global convergence of the proposed complex neural network models is theoretically proved. In addition, the efficacy and the superiority of the proposed complex neural network models is verified through illustrative computer-simulation examples.

In order to achieve our goal, it is necessary to provide explicit representations of WIPI as a particular outer inverse with prescribed range and null space. Therefore, our third goal is induced by the computational aspect of the WIPI and it investigates the full-rank and limiting representations of generalized inverses WIPI, WPPI, PPI, WMI and MI in relation to the full-rank representation of outer inverses with prescribed range and null space.

Our main results, enumerated according to the sequence of the sections, are as follows.

- (1) The WIPI, WPPI and WMI are represented as a particular outer inverse with prescribed range and null space.
- (2) An application of PPI in solving the indefinite least-squares problem is presented.
- (3) A new ZNN model, called ZNNWIPI, for computing the WIPI is derived using derived representations.
- (4) Convergence of the proposed ZNNWIPI model is investigated and numerical experiments are presented.

The global organization of the paper is as follows. Representations of the WIPI, WPPI and WMI and its main properties are investigated in Section 2. Application of the PI in solving indefinite least-squares problems is presented in Section 3. Using defined representations, corresponding ZNN models for computing the WIPI are developed in Section 4. Convergence analysis is presented in Section 5. Several illustrative numerical examples are presented in the last Section 6.

2. WIPI, WPPI AND PPI AS OUTER INVERSES

If $A \in \mathbb{C}_r^{m \times n}$ is $m \times n$ complex matrix of rank $\text{rank}(A) = r$, T is a subspace of \mathbb{C}^n of dimension $t \leq r$ and S is a subspace of \mathbb{C}^m of dimension $m - t$, then A has an outer inverse X with prescribed range $\mathcal{R}(X) = T$ and null space $\mathcal{N}(X) = S$ if and only if $AT \oplus S = \mathbb{C}^m$. In this case, X is unique and it is denoted by $A_{T,S}^{(2)}$. The outer generalized inverses with prescribed range and null-space have a remarkable significance in matrix theory. The $\{2\}$ -inverses have been used in the iterative methods for solving the nonlinear equations [1] as well as in statistics [5, 6]. In

particular, outer inverses show great influence in stable approximations of ill-posed problems and in linear and nonlinear problems involving rank-deficient generalized inverses [21, 51]. On the other hand, it is well known that the Moore-Penrose inverse A^\dagger and the weighted Moore-Penrose inverse $A_{M,N}^\dagger$, the Drazin inverse A^D and the group inverse $A^\#$ can be presented in a unique way, as generalized inverses $A_{T,S}^{(2)}$ for appropriate choice of matrices T and S [1]:

$$(7) \quad A^\dagger = A_{\mathcal{R}(A^*), \mathcal{N}(A^*)}^{(2)}, \quad A_{M,N}^\dagger = A_{\mathcal{R}(A^\dagger), \mathcal{N}(A^\dagger)}^{(2)}, \quad A^\# = N^{-1}A^*M.$$

For a given square matrix A the next identities are satisfied [1, 35, 39]:

$$(8) \quad A^D = A_{\mathcal{R}(A^k), \mathcal{N}(A^k)}^{(2)}, \quad k \geq \text{Ind}(A), \quad A^\# = A_{\mathcal{R}(A), \mathcal{N}(A)}^{(2)}.$$

Full-rank representation of $\{2\}$ -inverses with prescribed range and null space is determined in the next proposition, which was originated in [27].

Proposition 1. [27] *Let $A \in \mathbb{C}_r^{m \times n}$, T be a subspace of \mathbb{C}^n of dimension $s \leq r$ and let S be a subspace of \mathbb{C}^m of dimension $m - s$. In addition, suppose that $G \in \mathbb{C}^{n \times m}$ satisfies $\mathcal{R}(G) = T, \mathcal{N}(G) = S$. Let G has an arbitrary full-rank decomposition, that is $G = UV$. If A has a $\{2\}$ -inverse $A_{T,S}^{(2)}$, then:*

- (1) VAU is an invertible matrix;
- (2) $A_{T,S}^{(2)} = A_{\mathcal{R}(U), \mathcal{N}(V)}^{(2)} = U(VAU)^{-1}V$.

The following limit representation of outer inverses can be derived using the results from [17, 41].

Proposition 2. ([17, 18, 41]) *Let $A \in \mathbb{C}^{m \times n}$ be of rank r , let T be a subspace of \mathbb{C}^n of dimension $s \leq r$, and let S be a subspace of \mathbb{C}^m of dimension $m - s$. In addition, suppose that $G \in \mathbb{C}^{n \times m}$ satisfies $\mathcal{R}(G) = T$ and $\mathcal{N}(G) = S$. In the case of existence, $A_{T,S}^{(2)}$ can be derived using the following limit representation:*

$$(9) \quad A_{T,S}^{(2)} = \lim_{\lambda \rightarrow 0} (GA + \lambda I)^{-1}G.$$

Due to the representations given in Lemma 1, the WIPI can be considered as an outer inverse of prescribed range and null space. The spectrum of a complex matrix A is denoted by $\sigma(A)$.

Lemma 1. *Let $A = BC \in \mathbb{C}_r^{m \times n}$ be a full-rank factorization of rank A , $J_m \in \mathbb{C}^{m \times m}$, $J_n \in \mathbb{C}^{n \times n}$ be Hermitian involutions and $M \in \mathbb{C}^{m \times m}, N \in \mathbb{C}^{n \times n}$ be two Hermitian invertible matrices. Then $A_{M,N}^\circ$ exists if and only if $\text{rank}(AA^\approx) = \text{rank}(A^\approx A) = \text{rank}(A)$ and its full-rank representation is defined by*

$$(10) \quad \begin{aligned} A_{M,N}^\circ &= C^\approx (CC^\approx)^{-1} (B^\approx B)^\dagger B^\approx \\ &= C^\approx (B^\approx AC^\approx)^{-1} B^\approx \\ &= A_{\mathcal{R}(C^\approx), \mathcal{N}(B^\approx)}^{(2)} \\ &= A^\approx (A^\approx AA^\approx)^\dagger A^\approx. \end{aligned}$$

Proof. Firstly, one can verify that the result derived (for weighted Minkowski conjugate transpose) in [9] is valid for the weighted adjoint matrix A^\approx :

$$\sigma(A^\approx A) \text{ contains nonnegative real numbers} \iff \mathcal{N}(A^\approx A) = \mathcal{N}(A).$$

Further, using $\mathcal{N}(A^\approx A) = \mathcal{N}(A) \iff \text{rank}(AA^\approx) = \text{rank}(A)$, it follows that $\sigma(A^\approx A)$ contains nonnegative real numbers. Now, generalizing the limit representation of $A_{M,N}^\circ$ derived in [9], it can be verified that

$$(11) \quad A_{M,N}^\circ = \lim_{\lambda \rightarrow 0} (A^\approx A + \lambda I)^{-1} A^\approx = \lim_{\lambda \rightarrow 0} A^\approx (AA^\approx + \lambda I)^{-1}.$$

As a consequence, in view of Proposition 2, it follows that $A_{M,N}^\circ$ is a certain outer inverse with prescribed range and null space, as follows:

$$A_{M,N}^\circ = A_{\mathcal{R}(A^\approx), \mathcal{N}(A^\approx)}^{(2)}.$$

Now, the representations given in (10) can be obtained using basic representation of the outer inverse, presented in Proposition 1. \square

Corresponding representations of A° are derived in the next corollary.

Corollary 1. *Let $A = BC \in \mathbb{C}_r^{m \times n}$ be a full-rank factorization of A and $J_n \in \mathbb{C}^{n \times n}$, $J_m \in \mathbb{C}^{m \times m}$ be Hermitian involutions. Then A° exists if and only if $\text{rank}(AA^\sim) = \text{rank}(A^\sim A) = \text{rank}(A)$ and possess the following representations:*

$$(12) \quad \begin{aligned} A^\circ &= C^\sim (CC^\sim)^{-1} (B^\sim B)^{-1} B^\sim \\ &= C^\sim (B^\sim AC^\sim)^{-1} B^\sim \\ &= A_{\mathcal{R}(C^\sim), \mathcal{N}(B^\sim)}^{(2)} \\ &= A^\sim (A^\sim AA^\sim)^\dagger A^\sim \\ &= J_n (J_m A J_n)_{\mathcal{R}(C^*), \mathcal{N}(B^*)}^{(2)} J_m, \end{aligned}$$

where $A^\sim = J_n A^* J_m$.

Proof. It is necessary only the last representation. It follows from

$$\begin{aligned} A^\circ &= C^\sim (B^\sim AC^\sim)^{-1} B^\sim \\ &= J_n C^* J_r (J_r B^* J_m A J_n C^* J_r)^{-1} J_r B^* J_m \\ &= J_n C^* (B^* J_m A J_n C^*)^{-1} B^* J_m \end{aligned}$$

and $C^* (B^* J_m A J_n C^*)^{-1} B^* = (J_m A J_n)_{\mathcal{R}(C^*), \mathcal{N}(B^*)}^{(2)}$. \square

The particular choice $M = I_m, N = I_n, J_m = I_{1,m-1}, J_n = I_{1,n-1}$ in Corollary 1 leads to the full-rank representation of the MI, which was discovered in [52, Theorem 8]. Also, Lemma 1 in the case $J_m = I_m, J_n = I_n$ produces known representation of $A_{MN}^{(\dagger)}$, derived in [28, Theorem 3.2.]. This result is verified in Corollary 2.

Corollary 2. *Let $A = BC \in \mathbb{C}_r^{m \times n}$ be a full-rank factorization of rank r of the matrix A , let $J_m = I_m, J_n = I_n$ and M, N be two Hermitian invertible matrices of the order $m \times m$ and $n \times n$, respectively. Then $A_{MN}^{(\dagger)}$ exists if and only if $\text{rank}(AN^{-1}A^*M) = \text{rank}(N^{-1}A^*MA) = \text{rank}(A)$ and possess the following representations:*

$$(13) \quad A_{MN}^{(\dagger)} = N^{-1}C^* (CN^{-1}C^*)^{-1} (B^*MB)^{-1} B^*M.$$

Proof. Denote by N_r and M_r two Hermitian invertible matrices of the order $r \times r$. Then

$$C^\approx = N^{-1}I_n C^* I_r M_r = N^{-1}C^* M_r, \quad B^\approx = N_r^{-1} I_r B^* I_m M = N_r^{-1} B^* M.$$

Using the first representation of Corollary 1, one can obtain

$$\begin{aligned} A_{MN}^{(\dagger)} &= N^{-1}C^* M_r (N_r^{-1} B^* M A N^{-1} C^* M_r)^{-1} N_r^{-1} B^* M \\ &= N^{-1}C^* (B^* M A N^{-1} C^*)^{-1} B^* M, \end{aligned}$$

which was our original intention. \square

3. SOLVING INDEFINITE LEAST-SQUARES PROBLEMS USING PPI

The *indefinite matrix product* of two matrices $A \in \mathbb{C}^{m \times n}$ and $B \in \mathbb{C}^{n \times l}$ was introduced in [24] and defined by $A \circ B = A J_n B$, where $J_n \in \mathbb{C}^{n \times n}$ is a Hermitian involutory matrix. A matrix $A^{[\dagger]} \in \mathbb{C}^{n \times m}$ is called the Moore-Penrose inverse of $A \in \mathbb{C}^{m \times n}$ with respect to the indefinite matrix multiplication if it satisfies the following matrix equations:

$$A \circ X \circ A = A, \quad X \circ A \circ X = X, \quad (A \circ X)^\sim = A \circ X, \quad (X \circ A)^\sim = X \circ A.$$

The matrix $A^{[\dagger]}$ satisfies $A^{[\dagger]} = J_n A^\oplus J_m$ [24]. We will use the notation *indefinite matrix product pseudoinverse* (IMPPI) for $A^{[\dagger]}$.

The Moore-Penrose inverse in an indefinite inner product space when working with the usual matrix product exists if and only if $\text{rank}(AA^*) = \text{rank}(A^*A) = \text{rank}(A)$. It however exists in such spaces with the indefinite matrix product.

Corollary 3. *Let $A \in \mathbb{C}_r^{m \times n}$, $A = BC$ be a full-rank factorization of A and $J_m \in \mathbb{C}^{m \times m}$, $J_n \in \mathbb{C}^{n \times n}$ be two appropriate Hermitian involutions. Then $A^{[\dagger]}$ possesses the representation*

$$(14) \quad A^{[\dagger]} = C^* (C \circ C^*)^{-1} (B^* \circ B)^{-1} B^*.$$

Proof. The representation can be derived using the representations of A^\oplus from Corollary 1:

$$\begin{aligned} A^{[\dagger]} &= J_n A^\oplus J_m \\ &= J_n C^\sim (C C^\sim)^{-1} (B^\sim B)^{-1} B^\sim J_m \\ &= C^* J_r (J_r B^* J_m A J_n C^* J_r)^{-1} J_r B^* \\ &= C^* (B^* J_m A J_n C^*)^{-1} B^* \\ &= C^* (B^* \circ A \circ C^*)^{-1} B^* \\ &= C^* (C \circ C^*)^{-1} (B^* \circ B)^{-1} B^*. \end{aligned}$$

□

The investigation of indefinite least-squares problem (ILS problems) is restricted to real matrices. The solution of ILS problem of the general form

$$(15) \quad \min_x (Ax - b)^T J_m (Ax - b) = \min_x (Ax - b)^T \circ (Ax - b)$$

was investigated in [2]. The algorithm for finding the solution of (15) was proposed in [2] and it is based on the QR factorization of the coefficient matrix. This kind of problems arises in robust estimation, H^∞ -smoothing in estimation, filtering and control [2, 13]. Easily computable mixed and componentwise condition numbers of the ILS problem are presented in [13]. A solution of (15) which is based on the QR factorization of the coefficient matrix was proposed in [2]. In the current section, a correlation between the indefinite least-squares problem (15) and the pseudo-Euclidean generalized inverses is investigated. Further, our goal is to find solutions of the of indefinite least-squares problems

$$(16) \quad \min_x (Ax - b)^\sim \circ (Ax - b)$$

in terms of pseudo-Euclidean generalized inverses.

Theorem 1. *Let $A \in \mathbb{R}_n^{m \times n}$ and $J_m \in \mathbb{C}^{m \times m}$, $J_n \in \mathbb{C}^{n \times n}$ be two Hermitian involutions. The vector $J_n A^{[\dagger]} \circ b$ is the solution of the indefinite least-squares problem (15) if $A^T \circ A$ is symmetric positive-definite.*

Proof. According to known result from [2], the solution of (15) is the vector x_s given as the unique solution of the linear system of equations

$$(A^T J_m A)x_s = (A^T J_m b).$$

This implies

$$\begin{aligned} x_s &= (A^T J_m A)^{-1} A^T J_m b \\ &= (A^T \circ A)^{-1} A^T J_m b. \end{aligned}$$

The desired result follows from Corollary 3, in the case when $A^T \circ A$ is symmetric positive-definite. \square

Theorem 2. *Let $A \in \mathbb{R}_n^{m \times n}$. The vector $J_n A^\dagger b$ is the solution of the indefinite least-squares problem (16) if the matrix $A^T A$ is positive-definite.*

Proof. The normal equation corresponding to (16) is defined by

$$A^\sim \circ A \circ x = A^\sim \circ b.$$

The last equation can be rewritten in the equivalent form

$$J_n A^T J_m \circ A \circ x = J_n A^T J_m \circ b,$$

which gives

$$A^T J_m J_m A \circ x = A^T J_m J_m b \iff A^T A J_n x = A^T b.$$

If the matrix $A^T A$ is positive-definite, then

$$x = J_n (A^T A)^{-1} A^T b.$$

The proof can be completed using $A^\dagger = (A^T A)^{-1} A^T$. \square

4. ZNN MODELS FOR COMPUTING WEIGHTED INDEFINITE PSEUDOINVERSES

Our main idea is to modify complex underlying fundamental error-monitoring ZFs from [15, 49], and introduce general ZNN models which correspond to the time-varying WIPI. The limit representations given in (11) are useful in deriving the ZNN models for computing $A(t)_{M,N}^\circledast$. The limit representation originated in Lemma 2 can be derived extending (11) to time-varying complex matrix case and applying the result from [42]. For a better understanding of the statement, it is necessary to mention that the condition

$$\sigma \left(A^\sim (A^\sim A A^\sim)^* A^\sim |_{\mathcal{R}(A^\sim)} \right) \subset \Omega \subset (0, \infty)$$

is satisfied.

Lemma 2. Let $A(t) \in \mathbb{C}_r^{m \times n}$, $J_n \in \mathbb{C}^{n \times n}$, $J_m \in \mathbb{C}^{m \times m}$ be two appropriate Hermitian involutions and $M \in \mathbb{C}^{m \times m}$, $N \in \mathbb{C}^{n \times n}$ be two Hermitian invertible matrices. Then the WIPI of $A(t)$ is represented by the limit representations

$$(17) \quad A(t)_{M,N}^{\odot} = \lim_{\lambda \rightarrow 0} (A(t) \approx A(t) + \lambda I)^{-1} A(t) \approx = \lim_{\lambda \rightarrow 0} A(t) \approx (A(t)A(t) \approx + \lambda I)^{-1}.$$

$$(18) \quad A_{M,N}^{\odot} = \lim_{\lambda \rightarrow 0} (A(t) \approx (A(t) \approx A(t)A(t) \approx)^* A(t) \approx A + \lambda I)^{-1} A(t) \approx (A(t) \approx A(t)A(t) \approx)^* A(t) \approx \\ = \lim_{\lambda \rightarrow 0} A(t) \approx (A(t) \approx A(t)A(t) \approx)^* A(t) \approx (A(t)A(t) \approx (A(t) \approx A(t)A(t) \approx)^* A(t) \approx + \lambda I)^{-1}.$$

The starting point in defining the ZNN models for computing the WIPI arises from limit representations (17), (18) and two fundamental properties of $A(t)_{M,N}^{\odot}$ introduced in Lemma 3.

Lemma 3. Let $A(t) \in \mathbb{C}_r^{m \times n}$ be a given $m \times n$ matrix of rank r , let $J_m \in \mathbb{C}^{m \times m}$, $J_n \in \mathbb{C}^{n \times n}$ be two appropriate Hermitian involutions and $M \in \mathbb{C}^{m \times m}$, $N \in \mathbb{C}^{n \times n}$ be Hermitian invertible matrices. Then the matrix identities

$$(19) \quad \begin{aligned} A(t) \approx A(t)A(t)_{M,N}^{\odot} &= A(t) \approx, \\ A(t)_{M,N}^{\odot} A(t)A(t) \approx &= A(t) \approx \end{aligned}$$

are satisfied.

Proof. Firstly, using the representation of $A_{M,N}^{\odot} = A_{\mathcal{R}(A \approx), \mathcal{N}(A \approx)}^{(2)}$ from Lemma 1, one can verify the identities (cf. [4, 35]):

$$\begin{aligned} A(t)A(t)_{\mathcal{R}(A \approx), \mathcal{N}(A \approx)}^{(2)} &= P_{A \mathcal{R}(A \approx), \mathcal{N}(A \approx)}, \\ A(t)_{\mathcal{R}(A \approx), \mathcal{N}(A \approx)}^{(2)} A(t) &= P_{\mathcal{R}(A \approx), (A \approx \mathcal{N}(A \approx)^\perp)^\perp} \end{aligned}$$

the proof can be completed using known results:

$P_{L,M}G = G$ if and only if $\mathcal{R}(G) \subseteq L$ and $GP_{L,M} = G$ if and only if $\mathcal{N}(G) \supseteq M$. \square

4.1. The ZNNWIPI models

The complex ZNN model is developed by employing basic steps which were defined in [15, 37, 43].

According to the limit representations (9) and (18), it is reasonable to propose the following two dual fundamental error-monitoring ZFs which represent the basis for ZNN models appropriate for numerical computation of $A(t)_{M,N}^{\odot} = A(t)_{\mathcal{R}(A \approx), \mathcal{N}(A \approx)}^{(2)}$:

$$(20) \quad E^\approx(t) = \begin{cases} (G(t)A(t) + \lambda I) V_1(t) - G(t), & n \leq m, \\ V_1(t) (A(t)G(t) + \lambda I) - G(t), & n > m. \end{cases}$$

In (20), the parameter $\lambda > 0$ from (20) is sufficiently small and $G(t)$ is defined by (21)

$$G(t) = \begin{cases} A(t)^\approx, & \text{if the limit representation (9) is used,} \\ A(t)^\approx (A(t)^\approx A(t)A(t)^\approx)^* A(t)^\approx, & \text{if the limit representation (18) is used.} \end{cases}$$

Since (20) involves two dual cases, only the case $n \leq m$ is considered in details. The standard design formula is defined by

$$(22) \quad \dot{E}^\approx(t) := \frac{dE^\approx(t)}{dt} = -\gamma \mathcal{H}(E^\approx(t)),$$

where $\dot{E}^\approx(t)$ denotes the time derivative of $E^\approx(t)$, the scaling parameter $\gamma \in \mathbb{R}$, $\gamma > 0$, is as large as possible [15] and $\mathcal{H}(\cdot) : \mathbb{C}^{n \times m} \mapsto \mathbb{C}^{n \times m}$ is an appropriately defined complex-valued matrix-to-matrix activation function.

Two most popular activation functions from [14] will be exploited to develop (22). Let $C = A + \iota B = (c_{kj}) \in \mathbb{R}^{n \times m}$ be a complex matrix, where $\iota = \sqrt{-1}$ denotes the imaginary unit. Further, let $\mathcal{F}(D) = (f(d_{kj}))$ be a function element-wise applicable to elements of the complex matrix $D = (d_{kj}) \in \mathbb{R}^{n \times m}$, where $f(\cdot)$ is an odd and monotonically increasing function. The type I activation function is defined by

$$(23) \quad \mathcal{H}_1(C) = \mathcal{H}_1(A + \iota B) = \mathcal{F}(A) + \iota \mathcal{F}(B), \quad A, B \in \mathbb{R}^{n \times m}.$$

If $A \diamond B$ denotes the Hadamard product of matrices $A = (a_{ij}) \in \mathbb{R}^{n \times m}$ and $B = (b_{ij}) \in \mathbb{R}^{n \times m}$, i.e., $A \diamond B = (a_{ij}b_{ij})$, then the type II activation function is defined as

$$(24) \quad \mathcal{H}_2(C) = \mathcal{H}_2(A + \iota B) = \mathcal{F}(\Gamma) \diamond \exp(\iota \Theta),$$

where $\Gamma = |A + \iota B| \in \mathbb{R}^{n \times n}$ and $\Theta = \Theta(A + \iota B) \in (-\pi, \pi]^{n \times n}$ denote element-wise modulus and the element-wise arguments, respectively, of the complex matrix $C = A + \iota B$. The most widely used real-valued odd and monotonically increasing functions $f(x)$ are defined as follows.

Linear function: $f(x) = x$;

$$(a) \text{ Bipolar-sigmoid function: } f(x) = \frac{1 + \exp(-q)}{1 - \exp(-q)} \frac{1 - \exp(-qx)}{1 + \exp(-qx)}, \quad q > 2;$$

$$(b) \text{ Power-sigmoid function: } f(x) = \begin{cases} x^p, & \text{if } |x| \geq 1 \\ \frac{1 + \exp(-q)}{1 - \exp(-q)} \frac{1 - \exp(-qx)}{1 + \exp(-qx)}, & \text{otherwise} \end{cases}, \quad q \geq 2, p \geq 3;$$

$$(c) \text{ Smooth power-sigmoid function: } f(x) = \frac{1}{2}x^p + \frac{1 + \exp(-q)}{1 - \exp(-q)} \frac{1 - \exp(-qx)}{1 + \exp(-qx)}, \quad p \geq 3, q > 2.$$

To simplify notation, an universal mark \mathcal{H}_k will be used instead of \mathcal{H}_1 or \mathcal{H}_2 . The time derivative of $E^\approx(t)$ is equal to

$$(25) \quad \dot{E}^\approx(t) = \left(\dot{G}(t)A(t) + G(t)\dot{A}(t) \right) V_1(t) + (G(t)A(t) + \lambda I) \dot{V}_1(t) - \dot{G}(t).$$

Usage of (25) into the general ZNN pattern (22) with the general activation function \mathcal{H}_k leads to

$$(26) \quad \begin{aligned} (G(t)A(t) + \lambda I) \dot{V}_1(t) &= \dot{G}(t) - \left(\dot{G}(t)A(t) + G(t)\dot{A}(t) \right) V_1(t) \\ &\quad - \gamma \mathcal{H}_k \left((G(t)A(t) + \lambda I) V_1(t) - G(t) \right). \end{aligned}$$

Now, (26) can be transformed into the implicit ZNN model for computing $A(t)_{M,N}^{\odot}$:

$$(27) \quad \dot{V}_1(t) = \frac{1}{\lambda} \left[-G(t)A(t)\dot{V}_1(t) + \dot{G}(t) - \left(\dot{G}(t)A(t) + G(t)\dot{A}(t) \right) V_1(t) \right. \\ \left. - \gamma \mathcal{H}_k \left((G(t)A(t) + \lambda I) V_1(t) - G(t) \right) \right].$$

The ZNN model (27) designed for calculating the generalized inverse WIPI (resp. IPI, WPPI, PPI, WMI, MI) will be denoted by ZNNWIPI (resp. ZNNIPI, ZNNWPPI, ZNNPPI, ZNNWMI, ZNNMI). The general structure of the ZNNWIPI model is in the form of the union of a number of m independent subnetworks, wherein the j th subnetwork is aimed to approximation of the j th column $v_j(t)$ of $V_1(t)$, $j = 1, \dots, m$. Also, $g_j(t)$ denotes the j th column vector of the matrix $G(t)$. Then the dynamics of the j th subnetwork included into the ZNNWIPI network model can be expressed as

$$(28) \quad \dot{v}_j(t) = \frac{1}{\lambda} \left[-G(t)A(t)v_j(t) + \dot{g}_j(t) - \left(\dot{G}(t)A(t) + G(t)\dot{A}(t) \right) v_j(t) \right. \\ \left. - \gamma \mathcal{H}_k \left((G(t)A(t) + \lambda I) v_j(t) - g_j(t) \right) \right], \quad j = 1, \dots, m.$$

The model (28) is aimed to computation of v_j . Finally, the complex ZNN model (28) initiates the (ij) th neuron's dynamic equation in the form

$$(29) \quad \dot{v}_{ij} = \frac{1}{\lambda} \left[\sum_{k=1}^n b_{ik} \dot{v}_{kj} - \gamma \left(\sum_{k=1}^n \mathcal{H}_k (c_{ik} v_{kj} - g_{ij}) \right) - \sum_{k=1}^n d_{ik} v_{kj} + \dot{g}_{ij} \right],$$

wherein $i = 1, \dots, n$, $j = 1, \dots, m$ and

$$b_{ik} = (-G(t)A(t))_{ik}, \quad v_{kj} = (V_1(t))_{kj}, \quad c_{ik} = (G(t)A(t) + \lambda I)_{ik}, \\ d_{ik} = \left(\dot{G}(t)A(t) + G(t)\dot{A}(t) \right)_{ik}, \quad g_{ij} = (G(t))_{ij}.$$

Clearly, values of λ closer to zero lead to better approximation of the limiting representation (9).

4.2. Particular cases of ZNNWIPI and ZNNIPI

Case (1). The particular case $A(t)^\approx = A(t)^*$ of (20) gives the complex ZNN-II model derived in [15] with the aim of the pseudoinverse computation. The starting point in [15, 49] was the fact that the Moore-Penrose inverse $A(t)^\dagger$ which represents the left inverse satisfies the identity $A(t)^* A(t) A(t)^\dagger$. Further, on the basis of the assumption that $A(t)^* A(t)$ is invertible, the following matrix-based error function is considered

$$(30) \quad E(X(t), t) := A(t)^* A(t) X(t) - A(t)^*,$$

where $X(t)$ corresponds to the pseudoinverse inverse of $A(t)$. An elegant way to avoid the assumption of the invertibility of $A(t)^* A(t)$ was presented in [15]. Namely,

the authors of [15] defined the complex ZF, called ZF(5), which arises from the ZF defined in (30) and the Tikhonov regularization:

$$(31) \quad \bar{E}(X(t), t) = \left(A(t)^* A(t) + \lambda I \right) X(t) - A(t)^*, \quad \lambda > 0.$$

Clearly, (31) can be considered as the particular case $M = I_m, N = I_n, J_m = I_m, J_n = I_n$ of (20).

Case (2). The particular choice $M = I_m, N = I_n, J_m = I_{1,m-1}, J_n = I_{1,n-1}$ in (20) reduces the ZNNWIPI model into the ZNN model for computing the Minkowski inverse, called ZNNMI.

Case (3). In the case $M = J_m = I_m, N = J_n = I_n$, the ZNNWIPI model produces the ZNN model for computation of the Moore-Penrose inverse and the Moore-Penrose inverse in an indefinite inner product space which was introduced in [8], in the case of its existence.

Case (4). In the case when $J_m = I_m, J_n = I_n$ and M, N are two Hermitian invertible matrices of the order $m \times m$ and $n \times n$, respectively, the ZNNWIPI model produces the ZNN model for computation of the generalized weighted Moore-Penrose inverse $A_{MN}^{(\dagger)}$.

Case (5). In the most general case, J_m, J_n and M, N are arbitrary invertible matrices of appropriate orders. Then, according to (9), the ZNNWIPI model can be used in computation of the outer inverse the outer inverse

$$A(t)_{\mathcal{R}(A^\approx), \mathcal{N}(A^\approx)}^{(2)} = \lim_{\lambda \rightarrow 0} (A(t)^\approx A(t) + \lambda I)^{-1} A(t)^\approx.$$

Clearly, $A(t)_{\mathcal{R}(A^\approx), \mathcal{N}(A^\approx)}^{(2)}$ satisfies only the matrix equation (2).

5. CONVERGENCE ANALYSIS OF THE ZNNWIPI MODELS

Let us denote by ZNNWIPI-I the ZNN model which is based on the choice $G(t) = A(t)^\approx$ and by ZNNWIPI-II the ZNN model established upon the choice $G(t) = A(t)^\approx (A(t)^\approx A(t) A(t)^\approx)^* A(t)^\approx$. In this section, it is proven the global convergence of both the complex neural network models ZNNWIPI-I and ZNNWIPI-II. To simplify notation, by ZNNWIPI-I(1) and ZNNWIPI-I(2) we denote the model ZNNWIPI-I with the activation functions \mathcal{H}_1 or \mathcal{H}_2 , respectively.

5.1. Convergence of the models ZNNWIPI-I

The convergence properties of the complex ZNN models ZNNWIPI-I and ZNNWIPI-II, defined uniquely in (26), is investigated in this section.

Convergence of ZNNWIPI-I(1)

Theorem 3. *Assume that the time derivatives of the matrix $A(t) \in \mathbb{C}_r^{m \times n}$ exist and are continuous and uniformly bounded with respect to the time $t \in [0, +\infty]$. Let $J_m \in \mathbb{C}^{m \times m}$, $J_n \in \mathbb{C}^{n \times n}$ be two appropriate Hermitian involutions and let $M \in \mathbb{C}^{m \times m}$, $N \in \mathbb{C}^{n \times n}$ be two Hermitian invertible matrices. If the condition $\sigma(A(t) \approx A(t) |_{\mathcal{R}(A(t) \approx)}) \subset \Omega \subset (0, \infty)$ is satisfied, then the state matrix $V_1(t) \in \mathbb{C}^{n \times m}$ of the complex neural network model ZNNWIPI-I(1) globally converges to $A(t) \overset{\circ}{\ominus}_{M,N}$.*

Proof. Firstly, the limit representation (11) initiates

$$\begin{aligned} \lim_{\lambda \rightarrow 0} (A(t) \approx A(t) + \lambda I) A(t) \overset{\circ}{\ominus}_{M,N} &= \lim_{\lambda \rightarrow 0} (A(t) \approx A(t) + \lambda I) A(t) \overset{(2)}{\mathcal{R}(A(t) \approx), \mathcal{N}(A(t) \approx)} \\ &= A(t) \approx. \end{aligned}$$

Accordingly, if the replacement $\bar{V}_1(t) = V_1(t) - A(t) \overset{\oplus}{\ominus}_{M,N}$ is used, it follows that

$$\begin{aligned} \lim_{\lambda \rightarrow 0} E \approx(t) &= \lim_{\lambda \rightarrow 0} (A(t) \approx A(t) + \lambda I) V_1(t) - A(t) \approx \\ &= \lim_{\lambda \rightarrow 0} (A(t) \approx A(t) + \lambda I) V_1(t) - \lim_{\lambda \rightarrow 0} (A(t) \approx A(t) + \lambda I) A(t) \overset{\oplus}{\ominus}_{M,N} \\ &= \lim_{\lambda \rightarrow 0} (A(t) \approx A(t) + \lambda I) \bar{V}_1(t). \end{aligned}$$

Therefore, the ZF corresponding to $E \approx(t)$ can be defined as

$$E \approx(t) = (A(t) \approx A(t) + \lambda I) \bar{V}_1(t).$$

Then the general pattern $\dot{E} \approx(t) = -\gamma \mathcal{H}_1(E \approx(t))$ can be expanded into

$$\begin{aligned} (32) \quad & \left(\dot{A}(t) \approx A(t) + A(t) \approx \dot{A}(t) \right) \bar{V}_1(t) + (A(t) \approx A(t) + \lambda I) \dot{\bar{V}}_1(t) \\ & = -\gamma \mathcal{H}_1 \left((A(t) \approx A(t) + \lambda I) \bar{V}_1(t) \right). \end{aligned}$$

Since $E \approx(t) = \mathbf{Re}(E \approx(t)) + \iota \mathbf{Im}(E \approx(t))$, the general model $\dot{E} \approx(t) = -\gamma \mathcal{H}_1(E \approx(t))$ is equivalent to the following conjunctions of two equations in the real numbers domain:

$$\mathbf{Re}(\dot{E} \approx(t)) = -\gamma \mathcal{F}(\mathbf{Re}(E \approx(t))) \quad \text{and} \quad \mathbf{Im}(\dot{E} \approx(t)) = -\gamma \mathcal{F}(\mathbf{Im}(E \approx(t))).$$

The global convergence of ZNNWIPI-I(1) can be verified by means of the following Lyapunov function candidate:

$$(33) \quad L(t) = \frac{\|E \approx(t)\|_F^2}{2} = \frac{\text{Tr}(E \approx(t)^* E \approx(t))}{2}.$$

The time derivative of $L(t)$ satisfies the following identities:

$$\begin{aligned} \frac{dL(t)}{dt} &= \frac{\text{Tr} \left(\dot{E}^\approx(t)^* E^\approx(t) + E^\approx(t)^* \dot{E}^\approx(t) \right)}{2} \\ &= -\frac{1}{2} \gamma \text{Tr} \left\{ \left(\mathcal{F}(\mathbf{Re}(E^\approx(t)))^\top - \iota \mathcal{F}(\mathbf{Im}(E^\approx(t)))^\top \right) (\mathbf{Re}(E^\approx(t)) + \iota \mathbf{Im}(E^\approx(t))) \right. \\ &\quad \left. + \left(\mathbf{Re}(E^\approx(t))^\top - \iota \mathbf{Im}(E^\approx(t))^\top \right) (\mathcal{F}(\mathbf{Re}(E^\approx(t)))^\top + \iota \mathcal{F}(\mathbf{Im}(E^\approx(t)))) \right\} \\ &= -\gamma \text{Tr} \left\{ \mathbf{Re}(E^\approx(t))^\top \mathcal{F}(\mathbf{Re}(E^\approx(t))) + \mathbf{Im}(E^\approx(t))^\top \mathcal{F}(\mathbf{Im}(E^\approx(t))) \right\}. \end{aligned}$$

To make the presentation simpler, let us denote arbitrary (i, j) th element of $\mathbf{Re}(E^\approx(t))$ by e_{ij} and the (i, j) th element of $\mathbf{Im}(E^\approx(t))$ by e'_{ij} . Now, according to the assumption that the matrix function $\mathcal{F}(\cdot)$ is defined by an appropriate odd and monotonically increasing function $f(\cdot)$, it follows that

$$\begin{aligned} &\text{Tr} \left\{ \mathbf{Re}(E^\approx(t))^\top \mathcal{F}(\mathbf{Re}(E^\approx(t))) + \mathbf{Im}(E^\approx(t))^\top \mathcal{F}(\mathbf{Im}(E^\approx(t))) \right\} \\ &= \sum_j e_{ij} f(e_{ij}) + \sum_j e'_{ij} f(e'_{ij}) \geq 0 \end{aligned}$$

and finally

$$\frac{dL(t)}{dt} \begin{cases} < 0 & \text{if } E^\approx(t) \neq 0, \\ = 0 & \text{if } E^\approx(t) = 0. \end{cases}$$

As a conclusion, it follows that $\frac{dL(t)}{dt} \leq 0$ and $\frac{dL(t)}{dt} = 0$ if and only if $\bar{V}_1(t) = 0$. On the basis of the Lyapunov stability theory, $E^\approx(t) = (A(t)^\approx A(t) + \lambda I) V_1(t) - A(t)^\approx$ is globally convergent to zero. Therefore,

$$\lim_{\lambda \rightarrow 0} V_1(t) = \lim_{\lambda \rightarrow 0} (A(t)^\approx A(t) + \lambda I)^{-1} A(t)^\approx.$$

Based on the limiting representation (11), the state matrix $V_1(t)$ globally converges to $A(t)_{M,N}^\circ$ under the condition $\lambda \rightarrow 0$. \square

Convergence of ZNNWIPI-I(2)

Theorem 4. Assume that the time derivatives of the matrix $A(t) \in \mathbb{C}_r^{m \times n}$ exist and are continuous and uniformly bounded with respect to the time $t \in [0, +\infty]$. Let $J_m \in \mathbb{C}^{m \times m}$, $J_n \in \mathbb{C}^{n \times n}$ be two appropriate Hermitian involutions and let $M \in \mathbb{C}^{m \times m}$, let $N \in \mathbb{C}^{n \times n}$ be two Hermitian invertible matrices. If the condition $\sigma(A^\approx A |_{\mathcal{R}(A^\approx)}) \subset \Omega \subset (0, \infty)$ is satisfied, then the state matrix $V_1(t) \in \mathbb{C}^{n \times m}$ of the complex neural network model ZNNWIPI-I(2) is globally convergent to the time-varying outer inverse $A(t)_{M,N}^\circ$, starting from arbitrary initial state $V_1(0)$.

Proof. The dynamics initiated by the error function $E^\approx(t)$ is defined by the general pattern

$$\dot{E}^\approx(t) = -\gamma \mathcal{H}_2(E^\approx(t)).$$

Since $\mathcal{H}_2(E^\approx(t)) = \mathcal{F}(|E^\approx(t)|) \circ \exp(\iota\Theta(E^\approx(t)))$, the time derivative of the Lyapunov function candidate (33) is equal to

$$\begin{aligned} \frac{dL(t)}{dt} &= \frac{\text{Tr} \left(E^\approx(t)^* \dot{E}^\approx(t) + \dot{E}^\approx(t)^* E^\approx(t) \right)}{2} \\ &= -\frac{1}{2}\gamma \text{Tr} \left(E^\approx(t)^* \mathcal{H}_2(E^\approx(t)) + E^\approx(t) \mathcal{H}_2(E^\approx(t))^* \right) \\ &= -\frac{1}{2}\gamma \text{Tr} \left(E^\approx(t)^* \mathcal{H}_2(E^\approx(t)) + \left(E^\approx(t)^* \mathcal{H}_2(E^\approx(t)) \right)^* \right) \\ &= -\gamma \text{Tr} \left(\mathbf{Re} \left(E^\approx(t)^* \mathcal{H}_2(E^\approx(t)) \right) \right) \\ &= -\gamma \text{Tr} \left\{ \mathbf{Re} [E^\approx(t)^* \mathcal{F}(|E^\approx(t)|) \circ \exp(\iota\Theta(E^\approx(t)))] \right\}. \end{aligned}$$

Further, in view of $E^\approx(t) = |E^\approx(t)| \circ \exp(\iota\Theta(E^\approx(t)))$, it follows that

$$\frac{dL(t)}{dt} = -\gamma \text{Tr} \left\{ \mathbf{Re} [\exp(-\iota\Theta(E^\approx(t)^*)) \circ |E^\approx(t)^*|] (\mathcal{F}(|E^\approx(t)|) \circ \exp(\iota\Theta(E^\approx(t)))) \right\}.$$

Using once again that $\mathcal{F}(\cdot)$ is defined upon the element-wise usage of an odd and monotonically increasing function $f(\cdot)$, the inequality $\mathcal{F}(|E^\approx(t)|) \geq 0$, for $E^\approx(t) \neq 0$, can be concluded, which implies that the Lyapunov function $L(t)$ is negative definite. Therefore,

$$E^\approx(t) = (A(t)^\approx(t)A(t) + \lambda I)V_1(t) - A(t)^\approx$$

converges to the zero matrix starting from arbitrary initial value. Following the proof of Theorem 3, one can verify that the state matrix $V_1(t)$ globally converges to $A(t)_{M,N}^\circ$. \square

Convergence of ZNNWIPI-II

The model ZNNWIPI-II which is based on the usage of \mathcal{H}_1 or \mathcal{H}_2 is denoted by ZNNWIPI-II(1) or ZNNWIPI-II(2), respectively.

Theorem 5. *Assume that the time derivatives of the matrix $A(t) \in \mathbb{C}_r^{m \times n}$ exist and are continuous and uniformly bounded with respect to the time $t \in [0, +\infty]$. Let $J_m \in \mathbb{C}^{m \times m}$, $J_n \in \mathbb{C}^{n \times n}$ be two appropriate Hermitian involutions and $M \in \mathbb{C}^{m \times m}$, $N \in \mathbb{C}^{n \times n}$ be two Hermitian invertible matrices. Assume that the time derivatives of matrices $A(t)$ and $A(t)^\approx \in \mathbb{C}^{n \times m}$, $t \in [0, +\infty]$, exist and they are continuous and uniformly bounded with respect to the time t . Then the following statements are valid:*

- (a) *the state matrix $V_1(t) \in \mathbb{C}^{n \times m}$ of the complex neural network model ZNNWIPI-II(1) globally converges to $A(t)_{M,N}^\circ$.*
- (b) *the state matrix $V_1(t)$ of the complex neural network model ZNNWIPI-II(2) is globally convergent to the time-varying outer inverse $A(t)_{M,N}^\circ$.*

Proof. **(a)** The proof in this case can be completed using the limit representation (18) and following the proof of Theorem 3. In the essence, the proof is based on the same value $E^\approx(t)$ defined in (20), where $G(t)$ is defined in (21) as $G(t) = A(t)^\approx (A(t)^\approx A(t)A(t)^\approx)^* A(t)^\approx$ instead of $G(t) = A(t)^\approx$, used in the proof of Theorem 3.

(b) The second statement can be verified using the limit representation (18) and following the proof of Theorem 4. In the essence, the proof is based on the same value $E^\approx(t)$ defined in (20), where $G(t)$ is defined in (21) by the expression $G(t) = A(t)^\approx (A(t)^\approx A(t)A(t)^\approx)^* A(t)^\approx$ instead of $G(t) = A(t)^\approx$, used in the proof of Theorem 4. \square

6. NUMERICAL EXAMPLES

Example 1. **(a)** Consider the time varying matrix from [54]:

$$A(t) = S_3(t) = \begin{bmatrix} 1+t & t & 1+t \\ t^2 & -1+t & t \\ 1+t & t & 1+t \end{bmatrix}.$$

Our intention is to compute the outer inverse which correspond to the signature matrices

$$J_n = J_m = \begin{bmatrix} -1 & 0 & 0 \\ 0 & 1 & 0 \\ 0 & 0 & 1 \end{bmatrix} = I_{1,2}$$

and invertible matrices

$$M = \begin{bmatrix} 1 & 1 & 1 \\ 0 & 1 & 0 \\ 0 & 0 & 1 \end{bmatrix}, \quad N = \begin{bmatrix} 1 & 0 & 0 \\ 1 & 1 & 1 \\ 0 & 0 & 1 \end{bmatrix}.$$

It is easy to verify

$$A(t)^\approx = N^{-1}A^\sim M = N^{-1}J_n A^* J_m M = \begin{bmatrix} t+1 & -t^2+t+1 & 0 \\ -t & t^2-t-1 & 0 \\ -t-1 & -1 & 0 \end{bmatrix}.$$

Since

$$\text{rank}(A(t)^\approx A(t)) = \text{rank}(A(t)^\approx) = 2,$$

$A(t)_{\mathcal{R}(A^\approx), \mathcal{N}(A^\approx)}^{(2)}$ exists. Performing necessary computations in the package *Mathematica*, one can derive

$$\begin{aligned} A(t)_{\mathcal{R}(A^\approx), \mathcal{N}(A^\approx)}^{(2)} &= A(t)^\approx (A(t)^\approx A(t)A(t)^\approx)^\dagger A(t)^\approx \\ &= \begin{bmatrix} -\frac{t^3+t+1}{t^5+t^2} & \frac{t^2}{t^4-t^3+t-1} & 0 \\ \frac{1}{t^3-t^2+t} & \frac{1}{-t^2+t-1} & 0 \\ \frac{t^4+t+1}{t^5+t^2} & \frac{t}{-t^4+t^3-t+1} & 0 \end{bmatrix}. \end{aligned}$$

Let us choose the initial vector $v(0) = (1, 1, 1)^T$ and use the linear activation function. State variables trajectories of the complex model ZNNWPPI-I(1) with $\gamma = 10^8$ and $\lambda = 10^{-6}$ are shown in Figure 1 (a). Blue curves in this figure show the values corresponding to the solution computed by the model ZNNWPPI-I(1) and red curves display values corresponding to $A(t)_{M,N}^{\odot}$.

Residual errors

$$\left\| (A(t)_0^{\approx} A(t) + \lambda I) v_j(t) - a_{0j}^{\approx}(t) \right\|_2, \quad j = 1, 2, 3,$$

derived by ZNNWPPI-II(1) with $\gamma = 10^8$ and $\lambda = 10^{-6}$ are shown in Figure 2 (b), where red dots correspond to the linear function $f(\cdot)$, pink pluses indicate that $f(\cdot)$ is the power-sigmoid function with $p = 3$ and $q = 7$ and blue stars are corresponding to the bipolar-sigmoid function $f(\cdot)$ with $q = 10$.

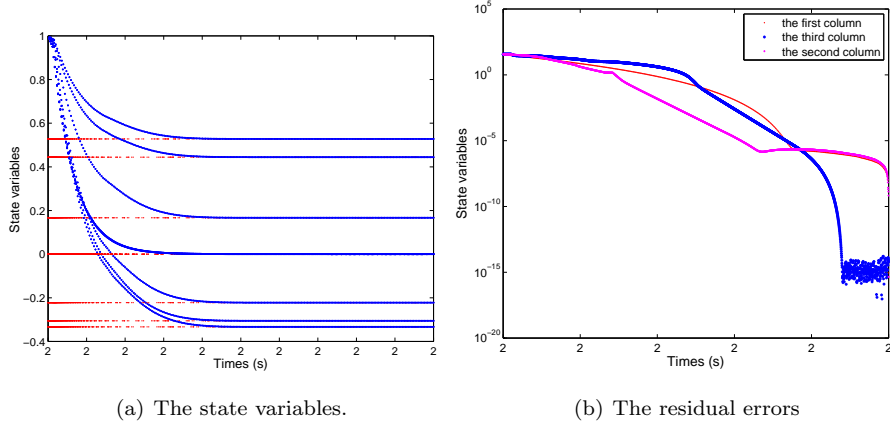


Figure 1: Trajectories of state variables and residual errors of ZNNWIPI-I(1) in Example 1, part (a).

In the following test, we consider the complex model ZNNWPPI-II(1) by using the matrix

$$A(t)_0^{\approx} = A(t)^{\approx} (A(t)^{\approx} A(t)^{\approx})^T A(t)^{\approx}.$$

Let us choose the initial vector $v(0) = (1, 1, 1)^T$ and use the linear activation function. State variables trajectories of the complex model ZNNWPPI-II(1) with $\gamma = 10^8$ and $\lambda = 10^{-6}$ are shown in Figure 2 (a). Blue curves in this figure show the values corresponding to the solution computed by the model ZNNWPPI-II(1) and red curves display values corresponding to the exact WPPI.

Residual errors

$$\left\| (A(t)_0^{\approx} A(t) + \lambda I) v_j(t) - a_{0j}^{\approx}(t) \right\|_2, \quad j = 1, 2, 3,$$

derived by ZNNWPPI-II(1) with the linear activation function, $\gamma = 10^8$ and $\lambda = 10^{-6}$ are shown in Figure 2 (b).

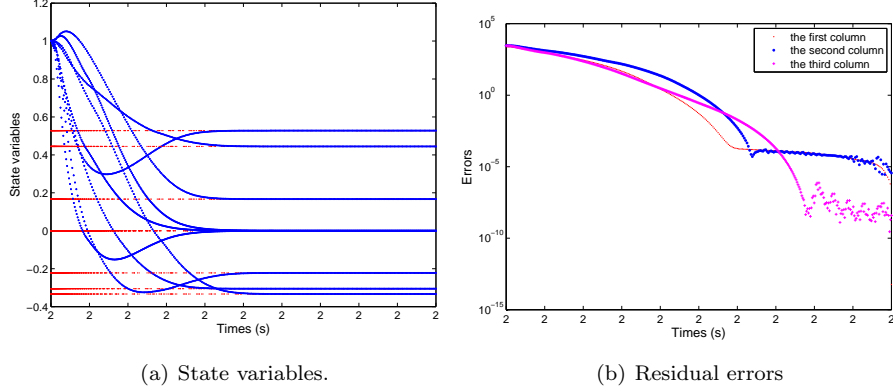


Figure 2: (a) Trajectories of state variables; (b) residual errors of ZNNWIPI-II(1) in Example 1, part (a).

(b) Further, let us choose $M = N = I$ and $J_m = J_n = I_{1,2}$. This implies

$$A(t)^\approx = A(t)^\sim = \begin{bmatrix} t+1 & -t^2 & -t-1 \\ -t & t-1 & t \\ -t-1 & t & t+1 \end{bmatrix}.$$

Performing necessary computations, one can verify

$$A(t)^{\mathcal{M}} = X(t) = A(t)^\sim (A(t)^\sim A(t)A(t)^\sim)^\dagger A(t)^\sim = \begin{bmatrix} -\frac{t^4(t+3)(t^3+t^2+t+3)}{t^{11}+t^{10}+t^9-t^8-4t^6+10t^5-18t^4+19t^3-13t^2+5t-1} & \frac{t^2(t^3+t^2+t+3)}{(t-1)(t^6+2t^5+t^4+3t^2-2t+1)} \\ \frac{t^2(t+3)(t^4+2t^3-2t^2+2t-1)}{t^{11}+t^{10}+t^9-t^8-4t^6+10t^5-18t^4+19t^3-13t^2+5t-1} & -\frac{t^4+2t^3-2t^2+2t-1}{(t-1)(t^6+2t^5+t^4+3t^2-2t+1)} \\ \frac{t^3(t+3)(t^3+3t^2+t+1)}{t^{11}+t^{10}+t^9-t^8-4t^6+10t^5-18t^4+19t^3-13t^2+5t-1} & -\frac{t(t^3+3t^2+t+1)}{(t-1)(t^6+2t^5+t^4+3t^2-2t+1)} \\ \frac{t^4(t+3)(t^3+t^2+t+3)}{t^{11}+t^{10}+t^9-t^8-4t^6+10t^5-18t^4+19t^3-13t^2+5t-1} & \\ -\frac{t^2(t+3)(t^4+2t^3-2t^2+2t-1)}{t^{11}+t^{10}+t^9-t^8-4t^6+10t^5-18t^4+19t^3-13t^2+5t-1} & \\ -\frac{t^3(t+3)(t^3+3t^2+t+1)}{t^{11}+t^{10}+t^9-t^8-4t^6+10t^5-18t^4+19t^3-13t^2+5t-1} & \end{bmatrix}.$$

Simple verification gives $\text{rank}(A(t)^\sim) = 2 > \text{rank}(X(t)) = 1$. Therefore, $X(t)$ does not represent the PPI of A . Later, one can verify

$$\text{rank}(A(t)^\sim A(t)A(t)^\sim) = 1 < \text{rank}(A(t)^\sim) = 2.$$

According to Urquhart's result [32],

$$X(t) \neq A(t)_{\mathcal{R}(A(t)^\sim), \mathcal{N}(A(t)^\sim)}^{(2)}.$$

Finally,

$$XAX = A^\sim (A^\sim AA^\sim)^\dagger A^\sim AA^\sim (A^\sim AA^\sim)^\dagger A^\sim = A^\sim (A^\sim AA^\sim)^\dagger A^\sim = X,$$

which means that X represents an outer inverse of A .

In such a case, the solution is to use the matrix

$$A_0^\sim = A^\sim (A^\sim AA^\sim)^\dagger A^\sim$$

instead of A^\sim . Let us choose the initial vector $v(0) = (1, 1, 1)^\top$, by using the linear function, state variables trajectories of the complex model ZNNPPI-I(1) with $\gamma = 10^8$ and $\lambda = 10^{-3}$ are shown in graphs included in Figure 3. Blue curves in this figure show the values corresponding to the solution computed by the model ZNNPPI-I(1) and red curves display values corresponding to the exact PPI. Resid-

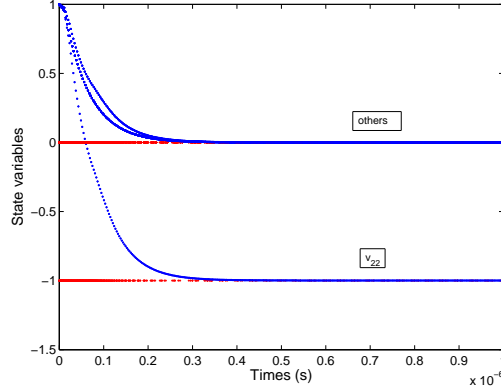


Figure 3: Trajectories of state variables in ZNNPPI-I(1) in Example 1, part (b).

ual errors

$$\left\| (A(t)_0^\sim A(t) + \lambda I) v_j(t) - a_0^\sim_j(t) \right\|_2, \quad j = 1, 2, 3,$$

derived by ZNNPPI-I(1) with $\gamma = 10^8$ and $\lambda = 10^{-6}$ are shown in Figure 4, where red dots correspond to the linear function $f(\cdot)$, pink pluses indicate that $f(\cdot)$ is the power-sigmoid function with $p = 5$ and $q = 7$, blue stars are corresponding to the bipolar-sigmoid function $f(\cdot)$ with $q = 5$ and green triangles indicate the smooth power-sigmoid function $f(\cdot)$ with $p = 5$ and $q = 11$, respectively.

(c) In the case $M = N = J_n = J_m = I$ (which implies $A^\sim = A^*$), the matrix $X(t)$ reduces to the Moore-Penrose inverse

$$A(t)^\dagger = \begin{bmatrix} \frac{-2t^4+2t^3-t+1}{4t^6-4t^5-2t^4+4t^3-2t^2+4} & -\frac{t^2(2t^2-1)}{-2t^6+2t^5+t^4-2t^3+t^2-2} & \frac{-2t^4+2t^3-t+1}{4t^6-4t^5-2t^4+4t^3-2t^2+4} \\ \frac{t(t^4-t^3+t+1)}{4t^6-4t^5-2t^4+4t^3-2t^2+4} & -\frac{-t^4+t^2-2t-2}{-2t^6+2t^5+t^4-2t^3+t^2-2} & \frac{t(t^4-t^3+t+1)}{4t^6-4t^5-2t^4+4t^3-2t^2+4} \\ \frac{t^5-t^3-t+1}{4t^6-4t^5-2t^4+4t^3-2t^2+4} & \frac{t(t^3+t^2-t-2)}{-2t^6+2t^5+t^4-2t^3+t^2-2} & \frac{t^5-t^3-t+1}{4t^6-4t^5-2t^4+4t^3-2t^2+4} \end{bmatrix}.$$

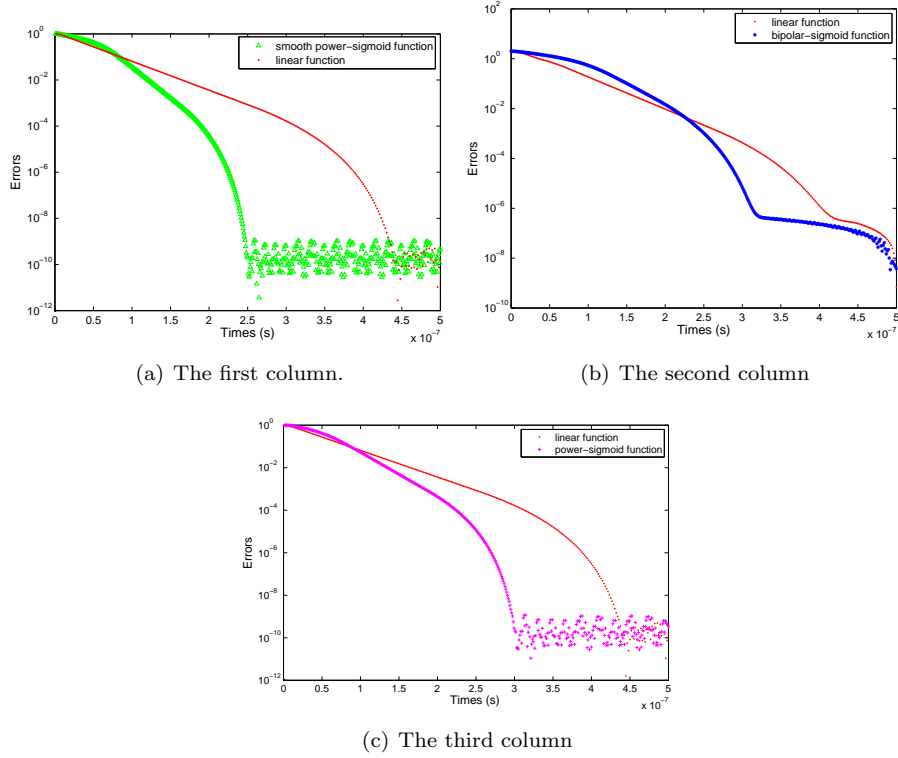


Figure 4: Trajectories of residual errors in ZNNPPI-I(1) in Example 1, part (b).

Let us now make numerical experiments corresponding to A^\dagger , the initial vector $v(0) = (1, 1, 1)^T$ and the linear function. State variables trajectories of the complex model ZNNPPI-I(1) with $\gamma = 10^8$ and $\lambda = 10^{-3}$ are shown in graphs included in Figure 5. Blue curves in this figure show the values corresponding to the solution computed by the model ZNNPPI-I(1) and red curves display values corresponding to the exact Moore-Penrose inverse.

Residual errors

$$\|(A(t) \approx A(t) + \lambda I) v_j(t) - a \approx_j(t)\|_2, \quad j = 1, 2, 3,$$

derived by ZNNPPI-I(1) with $\gamma = 10^8$ and $\lambda = 10^{-6}$ are shown in Figure 6, where red dots correspond to the linear function $f(\cdot)$, pink pluses indicate that $f(\cdot)$ is the power-sigmoid function with $p = 5$ and $q = 7$, blue stars are corresponding to the bipolar-sigmoid function $f(\cdot)$ with $q = 5$ and green triangles indicate the smooth power-sigmoid function $f(\cdot)$ with $p = 5$ and $q = 11$, respectively.

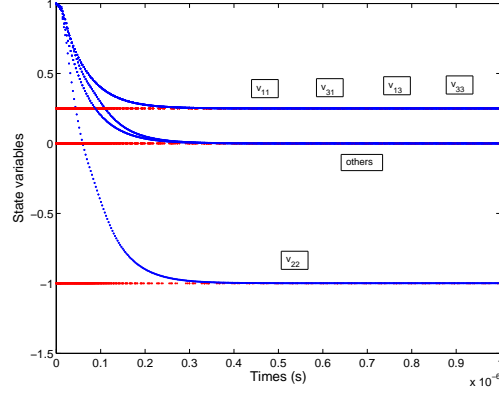


Figure 5: Trajectories of state variables in ZNNPI-I in Example 1, part (c).

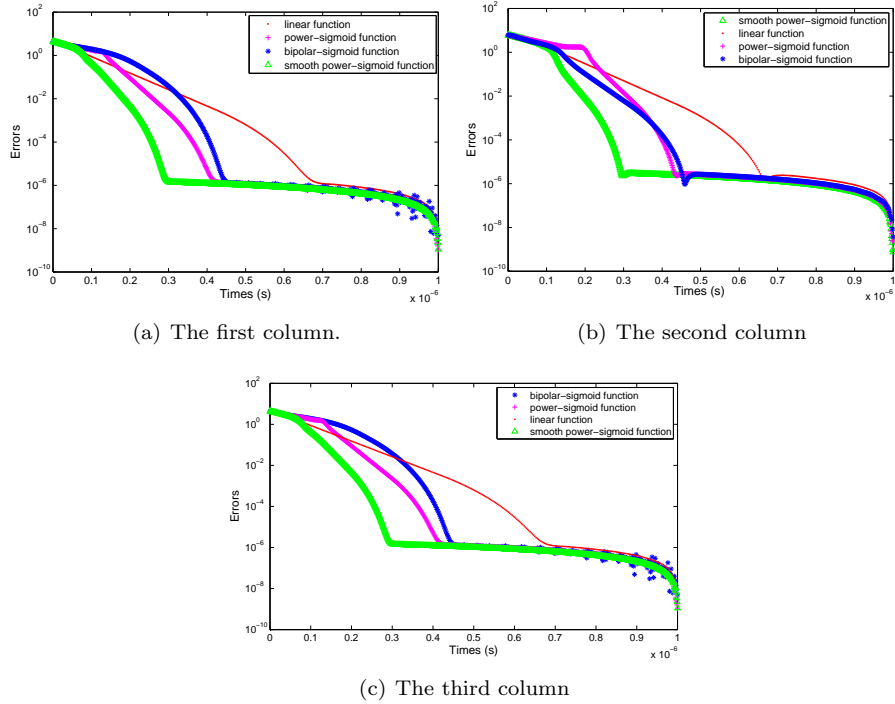


Figure 6: Trajectories of residual errors in ZNNPPI-I in Example 1, part (c).

Example 2. Let us consider the time-varying matrix

$$A(t) = \begin{bmatrix} i \sin(2t) & i \cos(2t) & -i \sin(2t) \\ -i \cos(2t) & i \sin(2t) & i \cos(2t) \\ i \sin(2t) & i \cos(2t) & 0 \end{bmatrix}$$

and choose

$$M = I_m, N = I_n, \quad J_n = J_m = \begin{bmatrix} -1 & 0 & 0 \\ 0 & 1 & 0 \\ 0 & 0 & 1 \end{bmatrix}.$$

Then

$$A(t)^\approx = A(t)^\sim = \begin{bmatrix} i \sin(2t) & i \cos(2t) & -i \sin(2t) \\ -i \cos(2t) & i \sin(2t) & i \cos(2t) \\ i \sin(2t) & i \cos(2t) & 0 \end{bmatrix}.$$

and

$$\begin{aligned} A(t)^\oplus &= A(t)^\sim (A(t)^\sim A(t) A(t)^\sim)^\dagger A(t)^\sim \\ &= \begin{bmatrix} \frac{1}{2} i \cos^2(2t) \csc(t) \sec(t) & i \cos(2t) & -i \csc(2t) \\ -i \cos(2t) & -i \sin(2t) & 0 \\ i \csc(2t) & 0 & -i \csc(2t) \end{bmatrix}, \end{aligned}$$

where

$$\csc(t) = 1/\sin(t), \quad \cot(t) = 1/\tan(t).$$

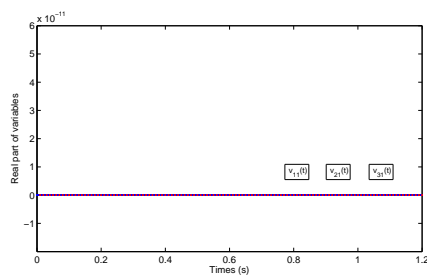
The Moore-Penrose inverse of $A(t)$, corresponding to the case $J_n = J_m = I$, is equal to

$$A(t)^\dagger = \begin{bmatrix} i \cos(2t) \cot(2t) & i \cos(2t) & -i \csc(2t) \\ -i \cos(2t) & -i \sin(2t) & 0 \\ i \csc(2t) & 0 & -i \csc(2t) \end{bmatrix}.$$

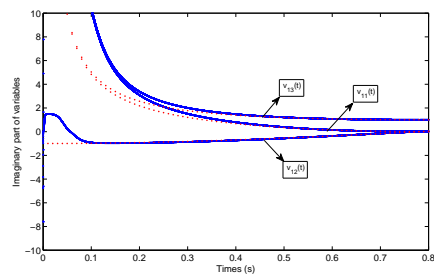
State variables trajectories derived by taking the initial vector $v(0) = (1, 1, 1)^T$ in the complex model ZNNMI(1) with $\gamma = 6 \times 10^4$ and $\lambda = 10^{-6}$ are displayed in graphs included in Figure 7. Blue curves in these figures show the values corresponding to the solution computed by the model ZNNMI-I(1) and red curves display values corresponding to the exact Minkowski inverse $A(t)^\oplus = A(t)^\mathcal{M}$. Figures 7 (a), (c) and (e) mean that real parts of all entries in the first, second and the third column, respectively, are zeros in this case.

Trajectories of residual errors $\|(A(t)^\approx A(t) + \lambda I) V(t) - A(t)^\approx\|_F$, generated by using the ZNNMI-I with type I activation functions, $\lambda = 10^{-3}$ and $\gamma = 10^6$ are shown in Figure 8 (a). The red dots mean that $f(\cdot)$ is linear, pink pluses denote power-sigmoid function $f(\cdot)$ with $p = 3$ and $q = 3$, blue stars indicate the choice of bipolar-sigmoid function $f(\cdot)$ with $q = 3$ and green triangles suggest that $f(\cdot)$ is smooth power-sigmoid function with $p = 3$ and $q = 5$, respectively.

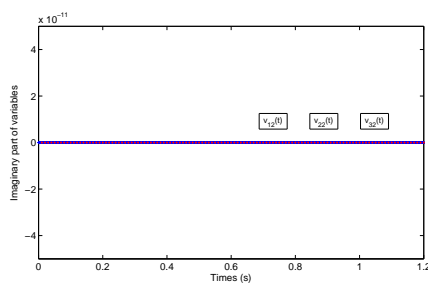
Trajectories of residual errors $\|(A(t)^\approx A(t) + \lambda I) V(t) - A(t)^\approx\|_F$, derived by employing the ZNNMI-I with type II activation functions, $\lambda = 10^{-3}$ and $\gamma = 10^6$ are shown in Figure 8 (b), where red dots indicate that $f(\cdot)$ is linear function, pink pluses denote the power-sigmoid function $f(\cdot)$ with $p = 3$ and $q = 5$, blue stars denote bipolar-sigmoid function $f(\cdot)$ with $q = 3$ and green triangles represent values derived by choosing the smooth power-sigmoid function $f(\cdot)$ with $p = 3$ and $q = 11$, respectively.



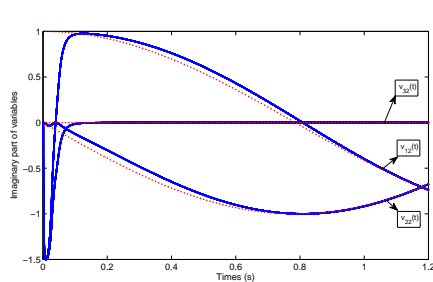
(a) Real part of the first column.



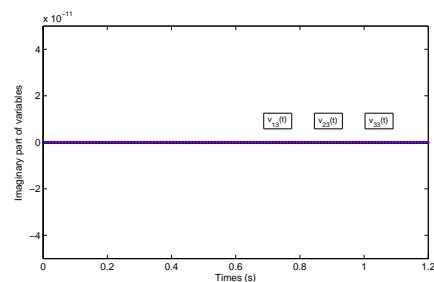
(b) Imaginary part of the first column.



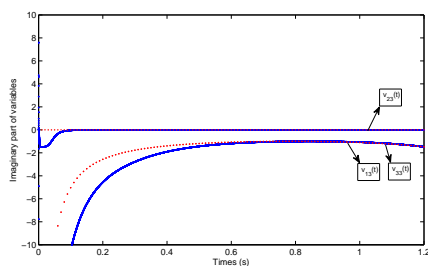
(c) Real part of the second column.



(d) Imaginary part of the second column.



(e) Real part of the third column.



(f) Imaginary part of the third column.

Figure 7: Trajectories of the state variables of the model ZNNMI-I(1) in Example 2.

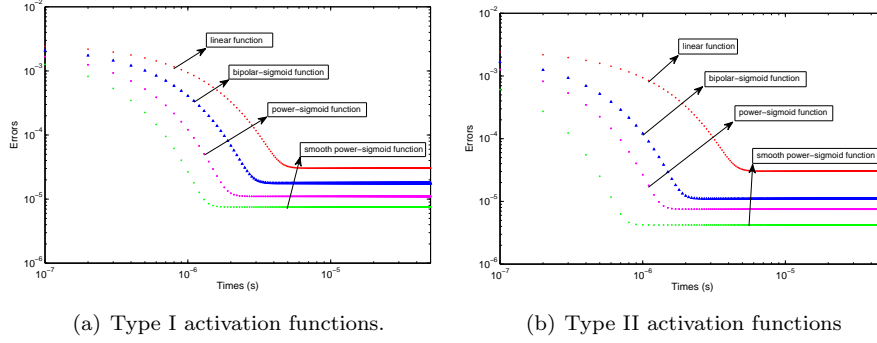


Figure 8: Trajectories of residual errors of ZNNMI-I with two types of activation functions in Example 2.

Example 3. Consider the matrix

$$A_6(t) = \begin{bmatrix} t+6 & t+5 & t+4 & t+3 & t+2 & t+1 \\ t+5 & t+5 & t+4 & t+3 & t+2 & t+1 \\ t+4 & t+4 & t+4 & t+3 & t+2 & t+1 \\ t+3 & t+3 & t+3 & t+3 & t+2 & t+1 \\ t+2 & t+2 & t+2 & t+2 & t+1 & t \\ t+1 & t+1 & t+1 & t+1 & t & t-1 \\ t & t & t & t & t-1 & t-2 \end{bmatrix}.$$

(a) In the case

$$J_n = \begin{bmatrix} -I_3 & 0 \\ 0 & I_3 \end{bmatrix}, J_m = \begin{bmatrix} -I_2 & 0 \\ 0 & I_5 \end{bmatrix}, N = I_6, M = I_7$$

the PPI of $A_6(t)$ is equal to

$$A_6(t)^\oplus = \begin{bmatrix} 1 & -1 & 0 & 0 & 0 & 0 & 0 \\ -1 & 2 & -1 & 0 & 0 & 0 & 0 \\ 0 & -1 & 2 & -\frac{7}{10} & -\frac{2}{5} & -\frac{1}{10} & \frac{1}{5} \\ 0 & 0 & -\frac{5}{6} & \frac{1}{60}(44-9t) & \frac{1}{60}(28-3t) & \frac{t+4}{20} & \frac{1}{60}(9t-4) \\ 0 & 0 & -\frac{1}{3} & \frac{1}{3} & \frac{1}{6} & 0 & -\frac{1}{6} \\ 0 & 0 & \frac{1}{6} & \frac{1}{60}(9t-4) & \frac{1}{60}(3t-8) & \frac{1}{20}(-t-4) & \frac{1}{60}(-9t-16) \end{bmatrix}.$$

The Moore-Penrose inverse of $A_6(t)$ is equal to $A_6(t)^\dagger = A_6(t)^\oplus$. Take the initial vector $v(0) = (0, 0, 0, 0, 0, 0)^T$. State variables trajectories of the ZNNPPI-I with $f(\cdot)$ is linear, $\gamma = 10^8$ and $\lambda = 10^{-6}$ are shown in Figure 9 (a).

Let $Z(t) = \|(A(t) \approx A(t) + \lambda I)V(t) - A(t) \approx\|_F$. Trajectories of relative errors $\frac{Z(t)}{Z(t)(1)}$, derived by employing the model ZNNPPI-I(1), $\lambda = 10^{-6}$ and $\gamma = 10^8$ are shown in Figure 9 (b), where $Z(t)(1)$ denotes the first component of $Z(t)$,

red dots indicate the linear function $f(\cdot)$, where red curves indicate that $f(\cdot)$ is linear function, pink curves denote the power-sigmoid function $f(\cdot)$ with $p = 5$ and $q = 10$, blue curves denote bipolar-sigmoid function $f(\cdot)$ with $q = 11$ and green curves represent values derived by choosing the smooth power-sigmoid function $f(\cdot)$ with $p = 7$ and $q = 11$, respectively.

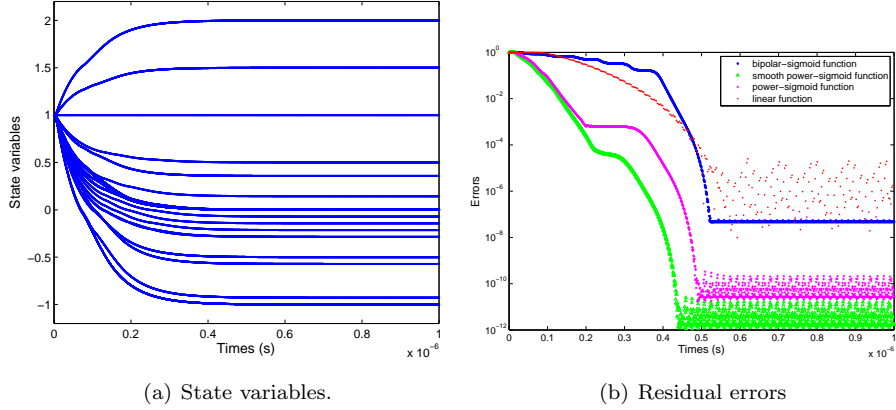


Figure 9: Trajectories of state variables and residual errors of the model ZNNPPI-I in Example 3, part (a).

(b) Further, continue Example 3 with the metric tensors chosen as

$$J_n = E(2, 5, 6) = \begin{bmatrix} 1 & 0 & 0 & 0 & 0 & 0 \\ 0 & 0 & 0 & 0 & 1 & 0 \\ 0 & 0 & 1 & 0 & 0 & 0 \\ 0 & 0 & 0 & 1 & 0 & 0 \\ 0 & 1 & 0 & 0 & 0 & 0 \\ 0 & 0 & 0 & 0 & 0 & 1 \end{bmatrix},$$

$$J_m = \begin{bmatrix} 1 & 0 & 0 & 0 & 0 & 0 & 0 \\ 0 & 1 & 0 & 0 & 0 & 0 & 0 \\ 0 & 0 & 1 & 0 & 0 & 0 & 0 \\ 0 & 0 & 0 & -1 & 0 & 0 & 0 \\ 0 & 0 & 0 & 0 & -1 & 0 & 0 \\ 0 & 0 & 0 & 0 & 0 & -1 & 0 \\ 0 & 0 & 0 & 0 & 0 & 0 & -1 \end{bmatrix} = I_{3,4}.$$

In this case,

$$A_6(t)^\odot = \begin{bmatrix} 1 & -1 & 0 & 0 & 0 & 0 & 0 \\ -1 & 2 & -1 & 0 & 0 & 0 & 0 \\ 0 & -1 & 2 & -\frac{7}{10} & -\frac{2}{5} & -\frac{1}{10} & \frac{1}{5} \\ -1 & 2 & -\frac{3}{2} & \frac{1}{20}(8-3t) & \frac{6-t}{20} & \frac{t+4}{20} & \frac{1}{20}(3t+2) \\ 2 & -4 & 1 & 1 & \frac{1}{2} & 0 & -\frac{1}{2} \\ -1 & 2 & -\frac{1}{2} & \frac{1}{20}(3t-8) & \frac{t-6}{20} & \frac{1}{20}(-t-4) & \frac{1}{20}(-3t-2) \end{bmatrix}.$$

Let $G(t) = A_0^\approx = A(t)^\approx (A(t)^\approx A(t)A(t)^\approx)^\top A(t)^\approx$. Take the initial vector $v(0) = (0, 0, 0, 0, 0, 0)^\top$. State variables trajectories of the ZNNPPI-II with $f(\cdot)$ is linear, $\gamma = 10^8$ and $\lambda = 10^{-6}$ are shown in Figure 10 (a).

Let $Z(t) = \|(G(t)A(t) + \lambda I)V(t) - G(t)^\approx\|_F$. Trajectories of relative errors $\frac{Z(t)}{Z(t)(1)}$, derived by employing the model ZNNPPI-II(1), $\lambda = 10^{-6}$ and $\gamma = 10^8$ are shown in Figure 10 (b), where $Z(t)(1)$ denotes the first component of $Z(t)$, red dots indicate the linear function $f(\cdot)$, where red curves indicate that $f(\cdot)$ is linear function, pink curves denote the power-sigmoid function $f(\cdot)$ with $p = 3$ and $q = 4$ and green curves represent values derived by choosing the smooth power-sigmoid function $f(\cdot)$ with $p = 7$ and $q = 11$, respectively.

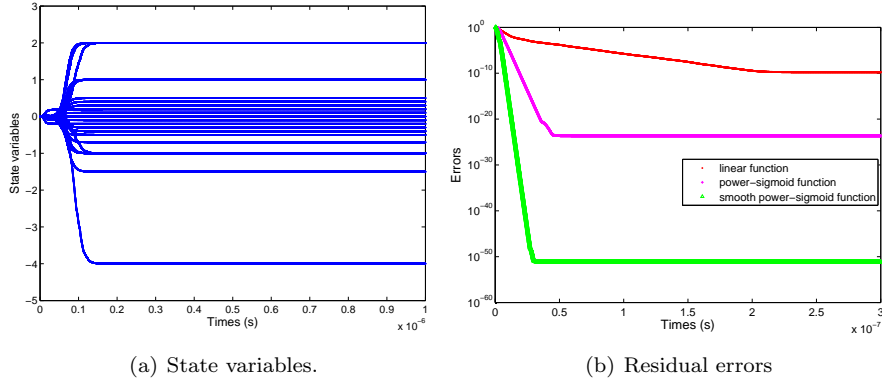


Figure 10: Trajectories of state variables and residual errors of ZNNPPI-II(1) in Example 3, part (b).

7. CONCLUSION

We investigate generalizations of Penrose equations in indefinite inner product spaces. Essentially, various generalizations of the weighted Moore-Penrose inverse are introduced, investigated and classified. In the widest sense, the notion

of the weighted indefinite pseudoinverse (WIPI) related to two Hermitian invertible matrices and two Hermitian involuntary matrices, is introduced. It is shown that various generalizations of the weighted Moore-Penrose inverse and the Moore-Penrose, so far considered in the literature, are appearances of the WIPI generalized inverses. In the case when Hermitian involuntary matrices become Minkowski matrices, the WIPI reduces to known notion of the weighted Minkowski inverse (WMI), investigated in [9, 53].

Full-rank and limit representations of the WIPI and the WMI are investigated. The WIPI and, particular, the WPPI and WMI are represented as a particular outer inverse with prescribed range and null space. Main properties of these generalized inverses are investigated.

An application of various pseudo-Euclidean pseudoinverses (PPI) in solving different types of indefinite least-squares problems is presented.

New ZNN model, called ZNNWIPI, for computing these generalized inverses is developed on the basis of full-rank and limiting representations of WIPI generalized inverses. Convergence behavior of the proposed ZNNWIPI model is investigated. Illustrative numerical results are presented.

Acknowledgements This project is supported by the bilateral project between China and Serbia “The theory of tensors, operator matrices and applications (no. 4-5)”.

Predrag Stanimirović gratefully acknowledge support from the Ministry of Education and Science, Republic of Serbia, Grant No. 174013.

Xue-Zhong Wang is supported by University research funding projects in Gansu province under grant 2014A-110 and National Natural Science Foundation of China under grants 11771099 and 11461020.

Haifeng Ma is supported by the bilateral project between China and Poland (no. 37-18).

REFERENCES

1. A. BEN-ISRAEL, T.N.E. GREVILLE: *Generalized Inverses: Theory and Applications*. Second Ed., Springer, 2003.
2. S. CHANDRASEKARAN, M. GU, A.H. SAYED: *A stable and efficient algorithm for the indefinite linear least-squares problem*. SIAM J. Matrix Anal. Appl. **20** (1998), 354–362.
3. A. CICHOCKI, T. KACZOREK, A. STAJNIAK: *Computation of the Drazin inverse of a singular matrix making use of neural networks*. Bulletin of the Polish Academy of Sciences Technical Sciences **40** (1992), 387–394.
4. Y. CHEN, B. ZHOU: *On g -inverses and nonsingularity of a bordered matrix $\begin{pmatrix} A & B \\ C & 0 \end{pmatrix}$* . Linear Algebra Appl. **133** (1990), 133–151.
5. A.J. GETSON, F.C. HSUAN: *$\{2\}$ -Inverses and their Statistical Applications*. Lecture Notes in Statistics 47, Springer, Berlin, 1988.
6. F. HUSEN, P. LANGENBERG, A. GETSON: *The $\{2\}$ -inverse with applications to statistics*. Linear Algebra Appl. **70** (1985), 241–248.

7. S. JAYARAMAN: *Nonnegative generalized inverses in indefinite inner product spaces*. Filomat **27** (2013), 659–670.
8. A. KAMARAJ, K.C. SIVAKUMAR: *Moore-Penrose inverse in an indefinite inner product space*. J. Appl. Math. Comput. **19** (2005), 297–310.
9. A. KILIÇMAN, ZEYAD AL ZHOUR: *The representation and approximation for the weighted Minkowski inverse in Minkowski space*. Math. Comput. Modelling **34** (2008), 363–371.
10. D. KRISHNASWAMY, G. PUNITHAVALLI: *The re-nnd definite solutions of the matrix equation $AXB = C$ in Minkowski space M* . Intern. J. Fuzzy Mathematical Archive, **2** (2013), 70–77.
11. D. KRISHNASWAMY, G. PUNITHAVALLI: *The anti-reflexive solutions of the matrix equation $AXB=C$ in Minkowski space M* . International Journal of Research and Reviews in Applied Sciences **15** (2013), 2–9.
12. D. KRISHNASWAMY, S. ANUSUYA: *Additive results on generalized Drazin inverse in Minkowski space M* . IOSR Journal of Mathematics (IOSR-JM) **12** (2016), 58–79.
13. H. LI, S. LI, H. YANG: *On mixed and componentwise condition numbers for indefinite least squares problem*. Linear Algebra Appl. **448** (2014), 104–129.
14. S. LI, Y. LI: *Nonlinearly activated neural network for solving time-varying complex Sylvester equation*. IEEE Trans. Cybern. **44** (2013), 1397–1407.
15. B. LIAO, Y. ZHANG: *Different complex ZFs leading to different complex ZNN models for time-varying complex generalized inverse matrices*. IEEE Trans. Neural Network Learn. Syst. **25** (2014), 1621–1631.
16. X. LIU, Y. QIN: *Iterative methods for computing the weighted Minkowski inverses of matrices in Minkowski space*. World Academy of Science, Engineering and Technology **75** (2011), 1083–1085.
17. X. LIU, Y. YU, J. ZHONG, Y. WEI: *Integral and limit representations of the outer inverse in Banach space*. Linear Multilinear Algebra **60** (2012), 333–347.
18. X. LIU, G. ZHU, G. ZHOU, Y. YU: *An analog of the adjugate matrix for the outer inverse $A_{T,S}^{(2)}$* . Math. Probl. Eng. **2012** Article ID 591256, 14 pages, doi:10.1155/2012/591256.
19. F. L. LUO, Z. BAO: *Neural network approach to computing matrix inversion*. Appl. Math. Comput. **47** (1992), 109–120.
20. A.R. MEENAKSHI: *Range symmetric matrices in Minkowski space*. Bull. Malays. Math. Sci. Soc. **23(1)** (2000), 45–52.
21. M.Z. NASHED: *Generalized Inverse and Applications*. Academic Press, New York, 1976.
22. Z. PENG, X. HU: *The reflexive and anti-reflexive solutions of the matrix equation $AX = B$* . Linear Algebra Appl. **375** (2003), 147–155.
23. M. PETROVIĆ, P.S. STANIMIROVIĆ: *Representations and computations of $\{2, 3^{\sim}\}$ and $\{2, 4^{\sim}\}$ -inverses in indefinite inner product spaces*. Appl. Math. Comput. **254** (2014), 157–171.
24. K. RAMANATHAN, K. KAMARAJ, K.C. SIVAKUMAR: *Indefinite product of matrices and applications to indefinite inner product spaces*. J. Anal. **12** (2004), 135–142.

25. K.A. REDDY, T. KURMAYYA: *Moore-Penrose inverses of Gram matrices leaving a cone invariant in an indefinite inner product space*. *Spec. Matrices* **3** (2015), 155–162.
26. M. RENARDY: *Singular value decomposition in Minkowski space*. *Linear Algebra Appl.* **236** (1996), 53–58.
27. X. SHENG, G. CHEN: *Full-rank representation of generalized inverse $A_{T,S}^{(2)}$ and its applications*. *Comput. Math. Appl.* **54** (2007), 1422–1430.
28. X. SHENG, G. CHEN: *The generalized weighted Moore-Penrose inverse*. *J. Appl. Math. & Computing* **25** (2007), 407–413.
29. P. S. STANIMIROVIĆ, I. S. ŽIVKOVIĆ, Y. WEI: *Recurrent neural network approach based on the integral representation of the Drazin inverse*. *Neural Computation* **27** (2015), 2107–2131.
30. P. S. STANIMIROVIĆ, I. S. ŽIVKOVIĆ, Y. WEI: *Recurrent neural network for computing the Drazin inverse*. *IEEE. Trans. Neural Network Learn. System* **26** (2015), 2830–2843.
31. P.S. STANIMIROVIĆ, I. ŽIVKOVIĆ, Y. WEI: *Neural network approach to computing outer inverses based on the full rank representation*. *Linear Algebra Appl.* **501** (2016), 344–362.
32. N.S. URQUHART: *Computation of generalized inverse matrices which satisfy specified conditions*, *SIAM Review* **10** (1968), 216–218.
33. J. WANG: *Recurrent neural networks for solving linear matrix equations*. *Comput. Math. Appl.* **26** (1993), 23–34.
34. J. WANG: *A Recurrent neural network for real-time matrix inversion*. *Appl. Math. Comput.* **55** (1993), 89–100.
35. G. WANG, Y. WEI, S. QIAO: *Generalized Inverses: Theory and Computations*. *Developments in Mathematics* 53. Singapore, Springer; Beijing, Science Press, 2018.
36. J. WANG: *Recurrent neural networks for computing pseudoinverses of rank-deficient matrices*. *SIAM J. Sci. Comput.*, **18** (1997), 1479–1493.
37. X.-Z. WANG, Y. WEI, P.S. STANIMIROVIĆ: *Complex neural network models for time-varying Drazin inverse*. *Neural Computation* **28** (2016), 2790–2824.
38. X.-Z. WANG, P.S. STANIMIROVIĆ, Y. WEI: *Complex ZFs for computing time-varying complex outer inverses*. *Neurocomputing* **275** (2018), 983–1001.
39. Y. WEI, P. S. STANIMIROVIĆ, M.D. PETKOVIĆ: *Numerical and Symbolic Computations of Generalized Inverses*. World Scientific Publishing Co. Pte. Ltd., Singapore, 2018.
40. Y. WEI: *Recurrent neural networks for computing weighted Moore–Penrose inverse*. *Appl. Math. Comput.* **116** (2000), 279–287.
41. Y. WEI: *A characterization and representation of the generalized inverse $A_{T,S}^{(2)}$ and its applications*. *Linear Algebra Appl.* **280** (1998), 79–86.
42. Y. WEI, N. ZHANG: *A note on the representation and approximation of the outer inverse $A_{T,S}^{(2)}$ of a matrix A* . *Appl. Math. Comput.* **147** (2004), 837–841.
43. Y. ZHANG, Y. YANG, N. TAN, B. CAI: *Zhang neural network solving for time-varying full-rank matrix Moore-Penrose inverse*. *Computing* **92** (2011), 97–121.

44. L. XIAO, B. LIAO: *A convergence-accelerated Zhang neural network and its solution application to Lyapunov equation*. Neurocomputing **193** (2016), 213–218.
45. Y. ZHANG, B. QIU, L. JIN, AND D. GUO: *Infinitely many Zhang functions resulting in various ZNN models for time-varying matrix inversion with link to Drazin inverse*. Information Processing Letters **115** (2015), 703–706.
46. Y. ZHANG, W. MA, B. CAI: *From Zhang neural network to Newton iteration for matrix inversion*. IEEE Transactions on Circuits and Systems **56** (2009), 1405–1415.
47. Y. ZHANG, S. SAM GE: *Design and analysis of a general recurrent neural network model for time-varying matrix inversion*. IEEE Transactions on Neural Networks **16** (2005), 1477–1490.
48. Y. ZHANG, C. YI, AND W. MA: *Simulation and verification of Zhang neural network for online time-varying matrix inversion*. Simulation Modelling Practice and Theory **17** (2009), 1603–1617.
49. Y. ZHANG, Z. LI, K. LI: *Complex-valued Zhang neural network for online complex-valued time-varying matrix inversion*. Appl. Math. Comput. **217** (2011), 10066–10073.
50. Y. ZHANG, Y. YANG, N. TAN, B. CAI: *Zhang neural network solving for time-varying full-rank matrix Moore-Penrose inverse*. Computing **92** (2011), 97–121.
51. B. ZHENG, R. B. BAPAT: *Generalized inverse $A_{T,S}^{(2)}$ and a rank equation*. Appl. Math. Comput. **155(2)** (2004), 407–415.
52. H. ZEKRAOUI, Z. AL-ZHOUR, CENAP ÖZEL: *Some new algebraic and topological properties of the Minkowski inverse in the Minkowski space*. The Scientific World Journal, Volume 2013, Article ID 765732, 6 pages.
53. Z. AL-ZHOUR: *Extension and generalization properties of the weighted Minkowski inverse in a Minkowski space for an arbitrary matrix*. Comput. Math. Appl. **70** (2015), 954–961.
54. G. ZIELKE: *Report on test matrices for generalized inverses*. Computing **36** (1986), 105–162.
55. I. ŽIVKOVIĆ, P.S. STANIMIROVIĆ, Y. WEI: *Recurrent neural network for computing outer inverse*. Neural Computation **28:5** (2016), 970–998.

Predrag S. Stanimirović

University of Niš,
Faculty of Sciences and Mathematics,
Višegradska 33, 18000 Niš,
Serbia
E-mail: *pecko@pmf.ni.ac.rs*

(Received 28.06.2017)

(Revised 05.11.2018)

Xue-Zhong Wang

School of Mathematics and Statistics,
Hexi University,
Zhangye, Gansu, 734000
P.R. China
E-mail: *xuezhongwang77@126.com*

Haifeng Ma

School of Mathematical Science,
Harbin Normal University,
Harbin 150025,
P. R. China E-mail: *haifengma@aliyun.com*